INVESTIGATING THE ABILITY OF CORAL REEFS TO PROTECT SHORELINES IN THE REPUBLIC OF KIRIBATI

by

Heather Summers

B.Sc., McMaster University, 2017

A THESIS SUBMITTED IN PARTIAL FULFILLMENT OF
THE REQUIREMENTS FOR THE DEGREE OF

MASTER OF SCIENCE
in
THE FACULTY OF GRADUATE AND POSTDOCTORAL STUDIES
(Geography)

THE UNIVERSITY OF BRITISH COLUMBIA
(Vancouver)

December 2019

The following individuals certify that they have read, and recommend to the Faculty of Graduate and Postdoctoral Studies for acceptance, a thesis entitled:

Investigating the ability of coral reefs to protect shorelines in the Republic of Kiribati

submitted by Heather Summers in partial fulfillment of the requirements for

the degree of Master of Science

in Geography

Examining Committee:

Dr. Simon Donner
Supervisor

Dr. Brett Eaton
Supervisory Committee Member

Dr. Marwan Hassan
Additional Examiner

Abstract

Coral reefs support a high biodiversity, providing a natural, physical barrier from waves that protects coastal communities from shoreline erosion and inundation. The three-dimensional (3D) structural complexity of living coral communities provides frictional resistance as waves and currents pass over the reef. A shift in coral community assemblages towards small, weedy, stress-tolerant corals due to climate change and local human stressors may alter wave attenuation, threatening low-lying coastal regions facing sea-level rise. In this thesis, I investigated the effect of coral community composition on shoreline protection in Kiribati's Tarawa and Abaiang Atolls by collecting fore reef and reef flat field data and creating 3D reconstructions of the fore reefs. I found that the 3D structure and contribution of certain coral growth forms to reef complexity varied depending on the complexity metric used. Surface rugosity and standard deviation of elevation were not significantly different between atolls, while the average terrain ruggedness was significantly greater at disturbed sites in South Tarawa dominated by the weedy species *Porites rus*. I show that the abundance of *Porites rus* and branching corals were positively related for all three complexity metrics, with the strongest positive association between *Porites rus* and terrain ruggedness. Lastly, I determined that South Tarawa reef flats, long mined of rocks for human use, have lower benthic roughness and receive higher offshore wave energy relative to North Tarawa. My research suggests that at current mean sea level, the difference in the diversity of coral growth forms on the fore reef across Tarawa and Abaiang have less effect on wave attenuation than other factors like coral cover, steepness of the fore reef, and benthic composition of the reef flat. Additionally, the most significant variation in wave runup will be due to parameters influencing fore reef slope and reef flat composition. As such, steeper fore reef slopes and smooth reef flats of South Tarawa are expected to dissipate less wave energy relative to reefs in North Tarawa and Abaiang. To summarize, my findings offer insights into possible trade-offs between reef resilience to climate change and shoreline protection, including shoreline vulnerabilities to sea-level rise around Kiribati.

Lay Summary

This thesis evaluated the role of coral community composition and reef physical structure on the ability of coral reefs to dissipate wave energy and protect the shorelines of two atolls, Tarawa and Abaiang, in the Republic of Kiribati. Analysis of three-dimensional models show that reefs around South Tarawa are impacted by human-related activities, such as sediments from causeway construction and poor waste management, whereas reefs around North Tarawa and Abaiang are less disturbed. Measurements based upon the models combined with data of their associated shorelines suggests that moderate coral cover, steep reefs, and smooth shorelines around South Tarawa offer less protection from erosion by waves relative to sites near North Tarawa and Abaiang. With rising sea levels due to climate change, understanding how the roughness of reefs and adjacent shorelines protect low-lying islands from flooding will help managers protect reef and shoreline features that reduce erosion by high energy waves.

Preface

The research objective for this dissertation was proposed by my supervisor Dr. Simon Donner (UBC), with whom I worked to design and execute the project. This dissertation draws from field work conducted around the Tarawa and Abaiang Atolls, Kiribati from April 12 to May 4, 2018. The field data presented in this dissertation was collected with the help of Dr. Donner and Sara Cannon, both from UBC, and Max Peter, Erietera Aram, and Toaea Beiateuea, who work for Kiribati's Ministry of Fisheries and Marine Resource Development (MFMRD). I was assisted by Sara Cannon in processing the benthic cover data from the quadrat photos. I completed all of the statistical analysis and processing of the photogrammetry data as well as the writing presented in this dissertation. Dr. Donner contributed to edits of this dissertation.

Table of Contents

List of Tables

List of Figures

List of Symbols

$\|r\|$	Resultant vector
cm	Centimetre
d_x	Increment in wave height decay
f_w	Friction factor
h_e	Depth of reef edge
H_o	Offshore wave height
h_r	Reef flat water depth
K_p	Reef profile factor
m	Metre
mm	Millimetre
n	Neighbourhood
n_r	Initial estimation of wave setup
W	Reef flat width
α	Slope
β	Aspect

List of Abbreviations

2D	Two-dimensional
3D	Three-dimensional
ACR	*Acropora*
AIC	Akaike information criterion
AIC_c	Second-order AIC
CoT	Crown-of-thorns starfish (*Acanthaster planci*)
CPCe	Coral Point Count with Excel Extensions
CV_{SST}	Coefficient of variation of maximum annual SST
DEM	Digital elevation model
ENSO	El Niño Southern Oscillation
FAV	*Favids*
GCP	Ground control point
HEL	*Heliopora*
LME	Linear mixed-effects
OA	Ocean acidification
OBC	Other branching coral
OMC	Other massive coral
PC1, PC2, …	Principal component axis 1, 2, …
PCA	Principal component analysis
POC	*Pocillopora*
PRM	*Porites* Massive
PRS	*Porites rus*
RVI	Relative variable importance
SDE	Standard deviation of elevation
SfM	Structure from motion
SST	Sea surface temperature

Acknowledgements

I would like to express my gratitude to my supervisor, Dr. Simon Donner, for his support, patience, and mentorship throughout my graduate studies. He always finds the time to listen to the challenges and obstacles that unavoidably crop up in the course of performing research and has taught me countless lessons and insights on the workings of academic research in general. I am grateful for the role Simon has played in providing me with workshops and projects that have allowed me to learn and experience more, both academically and personally, than I could have ever expected. My thanks also go to my committee member Dr. Brett Eaton, I am grateful for the discussions we have had and the many valuable comments shared.

I would also like to thank my lab group for their encouragement and support along the way, especially to Sara Cannon for her help in teaching me how to use CPCe and for her assistance in the field, I could not have asked for a better field partner. Thank you to Anya Leenman for teaching me the ins and outs of Agisoft PhotoScan, to Peter Whitman for his assistance with ArcGIS, and to Hugo Tello for his help creating the study site map. I am also grateful to NSERC for the funding that greatly aided travel to conferences and fieldwork.

This project would not have been possible without the support of the Fisheries Division of the Kiribati Ministry of Fisheries and Marine Resource Development (MFMRD). In particular, I would like to thank Max Peter, Erietera Aram, and Toaea Beiateuea of the MFMRD Research Unit for all of their support during field work, working many long days on land and at sea to ensure we were able to collect our data. I was very fortunate to be part of such a great field crew, their hard work and positive attitudes made my first trip to the Pacific Islands one I will never forget. I would also like to extend a huge thank you to Nabuti Mwemwenikarawa of the PIPA Trust and Eretia Monite of the Ministry of Education for organizing a cross-ministry workshop and for hosting us in North Tarawa so that we could complete the beach surveys. Lastly, I would like to thank Ariera Tekaata and the staff of Kiribati Sea Co. Ltd. who safely transported us to and from our dive sites and waited patiently while we collected our data.

I am also incredibly grateful to my family, especially my parents, Elizabeth and Peter, for their unwavering love and support in my pursuits and for instilling my interest in the natural sciences from an early age. Many thanks to Nick and Gay Ann Krischanowsky for their support throughout my MSc, especially the last few months. Thank you to my best friend Charlotte Tousaw for the endless hours talking on the phone and for always being there for me through the good times and the not so good times. Last, but not least, I have made some wonderful friends at UBC, in particular Elise Gallois, Mollie Holmberg, Cassandra Miller, Emily Adams, Jay Pahre, and Tiara Kerr. Thank you for all of your support and all the great experiences we have had including day hikes, evening beach swims, and pub nights.

Chapter 1: Introduction

Coral reefs are among the most ecologically productive and economically valued ecosystems, providing goods and services to humans through coastline protection, fisheries, tourism, and biochemical products (Hoegh-Guldberg et al., 2007). In the central equatorial Pacific Ocean people rely on coral reefs both for food and a means of protection from rising sea levels and high wave events driven by El Niño / Southern Oscillation events (ENSO; Solomon and Forbes, 1999). This confluence of rising sea level and high wave events threatens people who live on the Gilbert Islands of the Republic of Kiribati. Indeed, the atoll nation of Kiribati is considered to be the most vulnerable amongst nations in the world to deleterious impacts of sea-level rise including shoreline erosion, flooding of low-lying areas, and saline intrusion into the water table (Woodroffe, 2008; Webb and Kench, 2010; World Bank, 2013; Storlazzi et al., 2018). Current predictions of sea-level rise indicate possible submergence of many regions of Kiribati in the next century (Solomon and Forbes, 1999).

In recent decades the health of coral reef ecosystems has deteriorated due to compounding threats from sources that are global (ocean acidification (OA), global warming) and local (sedimentation, eutrophication, overfishing, proliferation of invasive species), leading to their reduced structural integrity and complexity (Williams et al., 2013). Structural complexity describes the roughness of the three-dimensional reef structure. A high structural complexity plays an important role in providing frictional resistance to waves and currents passing over the reef, significantly reducing wave energy that would otherwise directly impact shorelines (Rogers et al., 2016). Attenuation of wave energy by coral reefs can be significant. Ferrario et al. (2014) compiled a meta-analysis of published data relating to wave attenuation in coral reef environments and found that coral reefs reduce wave energy, on average, up to 97%.

The effectiveness of wave energy dissipation by coral reefs is likely to diminish under projected climate change scenarios. A reduction in shore protection can happen with increased atmospheric CO_2 concentration and sea surface temperature combined with a rise in mean sea level that could reduce the structural integrity, diversity, and overall health of corals. Few coral species are known to adapt to these changing environmental conditions (Sheppard et al., 2005; Hoegh-

Guldberg et al., 2007), with ongoing shifts in coral community assemblages toward stress-tolerant, weedy, low complexity species (Darling et al., 2017). Predicting the impact of reduced coral structural complexity and biodiversity on coastlines with greater confidence requires accurately evaluating how the structural complexity of these ecosystems responds to environmental changes (Burns et al., 2015). The focus of my research is to provide data on current coral reefs in Kiribati that can help predict future outcomes related to shoreline and island stability.

1.1 Literature Review

The importance of coral reef structural complexity in ecological functioning and the interaction of wave energy with reef structures have been the subject of considerable research (e.g., Quataert et al., 2015; Monismith et al., 2015; Costa et al., 2016; Osorio-Cano et al., 2017; Yao et al., 2019). These studies of coral structural complexity have shown that coral reefs act much like submerged breakwaters in that reefs lead to dramatic transformations in wave characteristics and subsequent rapid attenuation of wave energy (Kench and Brander, 2006; Ferrario et al., 2014). However, less is known about how the adverse impacts of climate change will effect coral reefs' ability to continue to provide effective wave attenuation and to protect coastal communities from rising sea levels.

1.1.1 Wave processes across a reef

In addition to the presence or absence of a reef, parameters such as reef dimensions, topography, and roughness (Spalding et al., 2014; Quataert et al., 2015; Kroeker et al., 2016) are characteristics that influence the wave height and wave energy dissipation across a reef (Brander et al., 2004; Kench and Brander, 2006). The detailed characteristics of wave transformation and energy dissipation across the forereef, reef crest, and reef flat have been studied for many years but the work to date has adopted a simple, two-dimensional treatment of windward reef platforms. The simplified models are limited by assumptions that wave transformations occur perpendicular to the reef crest and across reef structures with little to no consideration of significant topographic features (i.e. horizontal reef surface; Brander et al., 2004; Gourlay and Colleter, 2005; Jago et al., 2007) These simplifying assumptions are problematic in that reefs seldom meet these idealized forms; rather, there is morphologic variability between and within

reefs with regard to size, slope, and surface roughness. All of these morphologic parameters can influence wave processes acting across reef platforms (Kench and Brander, 2006).

The reef flat width, the distance between the reef crest and the shoreline, and water depth influence wave actions. Ferrario et al. (2014) reported that, on average, the reef flat is responsible for decreasing 65% of the offshore wave energy and 43% of the wave height. Kench and Brander (2006) reported that, on average, wider reef flats with a lower water depth dissipate a greater amount of the incident wave energy compared to narrow reef flats with a higher water depth. This determination is consistent with expectations because wider reef flats are able to dissipate more energy through bed friction. However, relatively narrow reef flats are also able to attenuate significant wave energy given that 50% of offshore wave energy attenuated over the reef flats occurs along the first 150 m of the zone. In addition, higher water levels on the reef flat result in an increase in the frequency and height of waves across the reef, thereby leading to increased swash on the beach (Quataert et al., 2015). Kench and Brander (2006) studied wave processes on Australian coral reefs and found that on the windward reefs of Lady Elliot Island there was no (0%) reduction in wave energy at higher tide levels compared to a 94% wave reduction at lower tide levels. As such, offshore water level, and subsequently water depth on the reef flat, exert significant control over energy dissipation across reefs.

Surface roughness also plays an important role in creating frictional drag as the waves and currents pass over the reef, significantly dampening wave action. The relative importance of friction on the reef flat is dependent upon the seaward reef slope. For coral reefs with a steep slope, bottom friction on the reef flat is negligible as a means of dissipating wave energy compared to turbulence. In contrast, bottom friction may be a significant factor in reducing wave energy for relatively flat reefs with waves breaking near the top of the fore reef (Massel and Gourlay, 2000; Gourlay and Colleter, 2005; Quataert et al., 2015). The surface roughness considers the topographic (i.e. structural) complexity of a coral reef structure, a feature that is correlated to substrate type (Nelson, 1996). Substrates such as sand offer very little friction compared to large, three-dimensional coral colonies that create large frictional forces important for wave attenuation (Spalding et al., 2014; Kroeker et al., 2016; Rogers et al., 2016). Using Gourlay's mathematical formulae (1996a, 1996b, 1997), Sheppard et al. (2005) examined their

data on Seychelles reefs to determine the effect of reef flat coral mortality on wave energy and propagation towards the shore. Simulation models predicted that a reduction in reef flat structural complexity of approximately 50% could double the wave energy reaching the shores behind the reefs with deleterious impacts on coastline stability (Sheppard et al., 2005).

It can generally be concluded that a higher bottom friction results in a decreasing wave runup, however, this deduction does not consider the influence of the fore reef zone. Quataert et al. (2015) studied a fore reef around Kwajalein Atoll, Republic of the Marshall Islands, characterized by a reef slope of approximately 5% and a rough morphology, and found that increased fore reef friction generates higher wave-induced set-up and thus results in more wave runup. The study by Monismith et al. (2015) contradicts this understanding as the authors found that a fore reef around Palmyra Atoll, U.S., characterized by a reef slope of approximately 9% and high coral cover (nearly 100% cover), thus high geometric complexity, provides greater shoreline protection than degraded fore reefs with low coral cover and low overall complexity. A challenge in studying the role of coral reefs in altering wave runup is that corals reefs are highly dynamic biophysical systems with varying morphologies and coral community compositions. However, a better understanding of coral species composition and their contribution to surface roughness and role in increasing wave attenuation is necessary as this knowledge would inform coral species use in reef restoration and conservation efforts (Ferrario et al., 2014).

1.1.2 Threats to a reef's ability to provide shoreline protection

Attenuation of wave energy by the surface roughness of a coral reef is essential for protecting and stabilizing tropical islands and mainland shores (Osorio-Cano et al., 2017). However, the effectiveness of wave energy dissipation is likely to diminish under projected climate change scenarios due to increased environmental stressors such as increases in ocean temperature, ocean acidification (OA), sea level rise, and local disturbances that influence the ability of a coral reef to deliver shoreline protection (Sheppard et al., 2005; Monismith et al., 2015; Quataert et al., 2015).

1.1.2.1 Increases in ocean temperature

Coral reefs are sensitive ecosystems that thrive under a narrow thermal interval, mostly due to the zooxanthellae, microalgae of the *Symbiodinium* genus, that live in symbiosis with the reef building corals, supplying up to 95% of their photosynthetic products to tissues of their coral hosts (Hoegh-Guldberg, 1999). Under stressful environmental conditions, such as elevated water temperatures (Heron et al., 2016; Hughes et al., 2017), a breakdown in the symbiosis between corals and their dinoflagellate can occur, a process known as coral bleaching. With prolonged loss of zooxanthellae, corals can experience partial or whole colony mortality, become more susceptible to diseases, and experience reduced photosynthesis, tissue growth, and calcification rates (Nyström et al., 2000; Baker et al., 2008; Perry and Morgan, 2017; Perry et al., 2018).

The extent of bleaching varies significantly depending on the severity of thermal stress, thermal history of the site, type and diversity of zooxanthellae, and environmental factors that influence irradiance, including water depth or turbidity, and water flow (Baker et al., 2008; Carilli et al., 2012; Guest et al., 2016; Donner and Carilli, 2019). Recent research suggests that corals that experience high temperature variability, have high energy reserves (i.e. lipids, carbohydrates, protein), and are less reliant on metabolites from symbionts may be able to adapt fast enough to keep up with the rate of environmental change (Baker et al., 2008; van Woesik et al., 2011; Schoepf et al., 2015). However, an increase in the frequency and intensity of thermal events as well as the compounding effects from human disturbance, has led to a shift towards smaller, stress-tolerant, weedy coral colonies that would reduce the overall structural complexity of the reefs (Alvarez-Filip et al., 2011; van Woesik et al., 2011; Alvarez-Filip et al., 2013; Darling et al., 2017). Magel et al. (2019) found similar results suggesting that coral mortality and reductions in coral accretion, reproduction, and recruitment that can follow global bleaching events are associated with a loss of reef structural complexity. Magel et al. (2019) created 3D reconstructions of fore reef plots around Kiritimati, Republic of Kiribati, and found that reef complexity, measured as surface rugosity and terrain ruggedness, declined one year after the 2015-2016 bleaching event. In addition, Graham and Nash (2013) and Alvarez-Filip et al. (2011) also found that coral cover was positively associated with reef structural complexity. Low levels of coral cover and decreased reef accretion may result in increased rates of erosion of the

underlying reef framework that can no longer be protected by growing corals (Alvarez-Filip et al., 2009).

The collapsing reef structure due to coral bleaching will cause a reduction in bottom friction thereby increasing wave energy and height (Sheppard et al., 2005; Quataert et al., 2015; Elliff and Silva, 2017). Sheppard et al. (2005) found that a loss of corals on the reef flat has led to increases in wave energy reaching coastlines for reefs in the Seychelles. Similarly, Monismith et al. (2015) studied a healthy fore reef (nearly 100% coral cover) around Palmyra Atoll and found that the complex canopy structure of the reef provided greater costal protection than a degraded reef. However, more research needs to be done on the effects of wave attenuation on fore reefs with low to moderate coral cover.

1.1.2.2 Ocean Acidification (OA)

An increase in atmospheric carbon dioxide (CO_2) and its subsequent sequestration by the oceans has led to a decrease in ocean pH and carbonate ions ($[CO_3^{2-}]$) needed by corals to construct their skeletons (Mollica et al., 2018). A study by Hoegh-Guldberg et al. (2007) predicts that if atmospheric CO_2 doubled that of pre-industrial levels, there would be a 40% reduction in coral calcification and growth resulting in less diverse coral communities and weakened carbonate reef structures. However, there have been mixed responses to the impact of OA on coral calcification in both lab experiments and field studies (Fabricius et al., 2011; Crook et al., 2013; Barkley et al., 2015; Enochs et al., 2015). Most studies estimate annual calcification rate based on annual linear extension and mean skeletal density. A study by Mollica et al. (2018) using *Porites* corals found that skeletal density is negatively affected by OA while extension is not, which may explain the large variability in the response of coral calcification to OA. The declines in coral skeletal density could increase the susceptibility of corals to bioerosion (Sammarco and Risk, 1990; Enochs et al., 2016; Schönberg et al., 2017), dissolution (van Woesik et al., 2013), and storm damage (Madin et al., 2012), thus compromising the ability of reefs to attenuate wave energy and protect islands from erosion.

1.1.2.3 Rising mean sea level

Sea-level rise and changing wave conditions are likely to have a negative impact on the capacity of coral reefs to protect shores (Quataert et al., 2015; Saunders et al., 2015; Perry et al., 2018). Sea-level patterns driven by ENSO events in the central and southwest Pacific over the last 50 to 100 years have shown large inter-annual variations of ± 0.45 m in sea-level (Church et al., 2006). In addition to these short term oscillations there is a long term trend in sea-level rise of approximately 1.6 mm per year, consistent with global projections (Church et al., 2006; Webb and Kench, 2010). Increased sea-level coupled with slow or nonexistent reef growth may lead to "drowned" reefs in which the submerged corals will fail to thrive under rising sea-level (Hoegh-Guldberg et al., 2007). Net accretion of reefs cease when rates of erosion exceed the rates of growth and recruitment, resulting in the flattening of reefs with reduced overall complexity and decreased capacity to attenuate offshore wave energy (Principe et al., 2012). Moreover, sea-level rise is expected to raise mean water depths on reef flats thereby allowing higher wave energy to propagate onto reef surfaces resulting in increased erosion of coastal shorelines (Sheppard et al., 2005).

Based on current projections of sea-level rise, many low-lying atoll islands, such as the Republic of Kiribati in the central equatorial Pacific Ocean, are expected to be negatively impacted by rising sea-level including shoreline erosion, flooding of low-lying areas, and contamination of the limited supply of drinking water (Webb and Kench, 2010; Storlazzi et al., 2018). Some scientists propose that island erosion may become widespread resulting in the submergence of entire atoll nations in the next century (Solomon and Forbes, 1999) with consequent threats to large segments of the population of these nations. In contrast, other researchers challenge the perceptions of island loss and suggest that shorelines should continue to build even with increased sea-level (Kench et al., 2018; Duvat, 2019), as long as there is sediment supply from the accretion and breakdown of coral reefs (Kench and Cowell, 2001). Webb and Kench (2010) studied the morphological variability of 27 Pacific atolls and found that many of the reef islands remained stable or even increased in size in the past 20 to 60 years despite rising sea-levels. It is anticipated that the rate, mode, and magnitude of geomorphic change is likely to increase with future increases in sea-level. However, there has been no recent study that examines decadal-scale adjustments in response to current variations in sea-level. Due to the high spatial and

temporal variability in coastal erosion and deposition processes, the timescale by which changes in sea-level will influence coral reef accretion and shoreline protection is uncertain.

1.1.2.4 Local threats

The ecosystem service of shoreline protection can also be greatly impeded by local human impacts, such as pollution, sedimentation, overfishing, and other forms of environmental degradation. The effect of local stressors on coral reefs depends on the features of each reef, including proximity to villages, coral species composition, reef bathymetry, and wave energy (i.e. water flushing rates and currents).

Sedimentation can be caused by human activities such as construction that free up sediments that are then washed into reefs. Sediment can smother corals, and the increased turbidity can prevent the corals from feeding or reduce the capacity of their zooxanthellae to photosynthesize (Weber et al., 2012). In South Tarawa, the construction of causeways linking the islets has limited the exchange of water between the lagoon and open ocean which has altered sediment deposition patterns and reduced water quality (Donner and Carilli, 2019). In addition to temperature threats and sedimentation, South Tarawa has a high population density and experiences high nutrient pollution due to poor overall waste management. Kiribati's Gilbert Islands also recently experienced an outbreak of *Acanthaster planci* ("Crown-of-Thorns" starfish) in 2013 and 2014 (Donner, unpublished data), that included Tarawa and Abaiang Atolls. Crown-of-thorns starfish (CoT) feed on reef-building corals, and in high numbers can decimate coral reefs (Kayal et al., 2012), resulting in a decline in reef complexity, coral cover, and biodiversity, and thus reduced wave attenuation. A study by Brodie et al. (2005) of *A. planci* larval development on the Great Barrier Reef found a link between increased nutrient runoff from land and *A. planci* outbreaks, although it is unclear whether nutrients influenced the CoT outbreak in Kiribati.

1.2 Research Summary and Objectives

Typically, each year the world's coral reefs experience high seasonality but only moderate variability in the maximum sea surface temperature (SST) reached. However, the interannual range in SSTs for coral reefs in the Republic of Kiribati exceed the seasonal range by two to six times (Donner, 2011). This unique mode of temperature variability largely only occurs in the

central equatorial Pacific. Coral reefs in Kiribati's Gilbert Islands may be relatively resilient to heat stress due to this unique temperature experience (Carilli et al., 2012). Moreover, a study by Donner and Carilli (2019) found that bleaching resistance is highest at the most disturbed reefs that feature low coral biodiversity and were observed to have a low reef structural complexity. These observations suggest a possible trade-off between reef resilience to climate change and reef's ability to attenuate waves, a key concern for atoll nations coping with the compounding effects of ocean acidification, increased SST, sea-level rise, and local disturbance.

The overarching goal of my thesis was to understand the potential impacts of disturbed coral assemblages that undergo shifts in composition towards stress-tolerant, weedy species on the capacity of a reef to protect shorelines. To investigate the effect of differences in coral community composition on shoreline protection, I compared the benthic cover and structural complexity from 3D reconstructions of the fore reefs and reef flat roughness observations taken across field sites around Tarawa and Abaiang Atolls. I then used a simple model to estimate the effect of different observed fore reef and reef flat characteristics on wave attention. I hypothesized that the highly disturbed, *Porites rus*-dominated South Tarawa sites would exhibit a low fore reef structural complexity and low bottom roughness on the reef flat and, as a result, would exhibit reduced wave attenuation across the reefs resulting in low shoreline protection.

Tarawa and Abaiang Atolls in the Republic of Kiribati presented an ideal location to investigate our hypothesis, as they provide a natural laboratory where the close proximity of the atolls and similarities in oceanographic conditions allowed us to compare the complexity of fore reefs and reef flats across a gradient of human impacts while reducing potential confounding factors. In addition, the interannual temperature variability of the Tarawa and Abaiang Atolls provides an environment with coral reefs exposed to elevated ocean temperatures and hence an opportunity to envision what reefs elsewhere may look like in a future of higher ocean temperatures.

Chapter 2: Methods and Materials

2.1 Study site selection: location and features

In April and May 2018, three dimensional (3D) reef structure was surveyed for 16 fore reef sites around the Republic of Kiribati's Tarawa (1°30' N, 173° E) and Abaiang (1°50' N, 173° E) Atolls in the central equatorial Pacific (Figure 2.1, Table A.1). The selected atolls are narrow and, on average, only 2 m above mean sea level (Woodroffe, 2008; Aung et al., 2009). The field sites were chosen based on previous surveys, diversity of human disturbance and reef environments, and accessibility. The surveyed sites are predominantly located on the southern and western reefs where they are protected from prevailing winds and waves and as such are safer to access (Donner, Kirata and Vieux, 2010; Donner and Carilli, 2019). However, two sites (T05 and T16) are located on coral reef environments with high exposure to prevailing winds and waves. A local human disturbance metric was calculated for each site as the natural logarithm of the population of the nearest village divided by the distance to the center of the nearest village (Carilli and Walsh, 2012; Ministry of Finance and Economic Development, 2016).

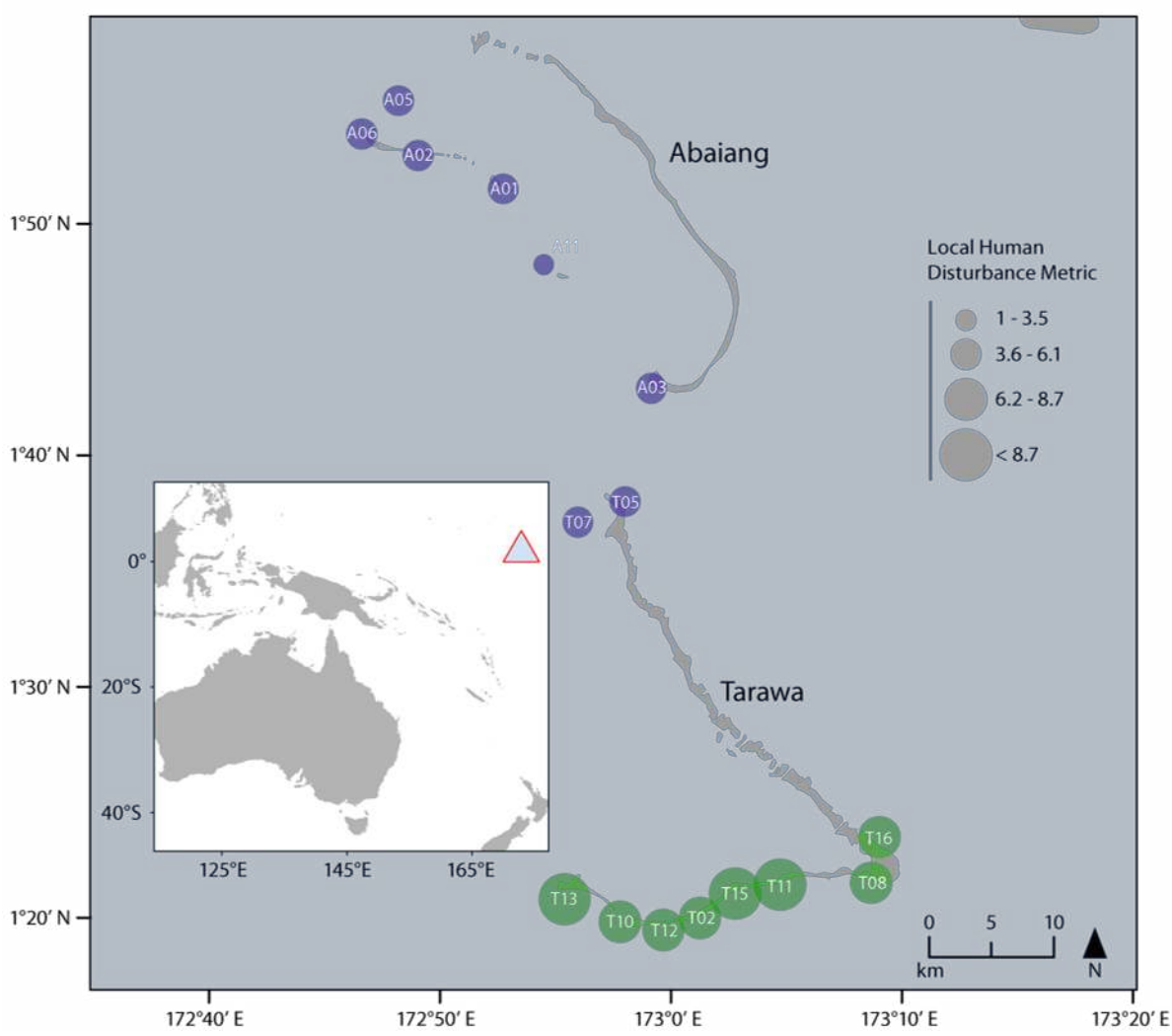

Figure 2.1 – Map of fore reef study sites around Tarawa and Abaiang, Republic of Kiribati. Sites in South Tarawa are shown in green and sites in North Tarawa and Abaiang are shown in purple. The sites are divided into three levels of local human disturbance metric. Inset shows the location of the Republic of Kiribati's Tarawa and Abaiang Atolls in the central equatorial Pacific Ocean.

2.2 Benthic composition

The benthic cover analysis followed an established protocol for monitoring in Kiribati. Benthic composition and coral size structure were quantified at each site using a 50 m transect tape randomly laid along the fore reef at 10 m depth (Buglass et al., 2016; Cannon et al., 2019). At 50 cm intervals along the transect, 0.33 m^2- sized quadrat photos were taken (50.0 cm width by 66.7 cm length) for a total of 100 photos per site. In addition, the length (in cm) of hard corals within 25 cm of either side of the transect tape were measured *in situ* following protocols reported by Cannon et al. (2019). Quadrat photos from the transects were processed using Coral Point Count

with Excel Extensions (CPCe) Research Software (version 4.1; Kohler and Gill, 2006). Benthic cover was manually identified at 20 points in each photo, leading to 2000 points per transect, following methods used in Cannon et al. (2019) and previous Kiribati surveys. The benthic cover was categorized to the genus level for coral (with the exception of *Porites rus*) and macroalgae, and to functional groups for sponges, soft coral, algal turf, crustose coralline algae, and cyanobacteria. *Porites rus* was identified to the species level because it is the one common encrusting *Porites* species in the region and has been identified as dominant in previous work (Donner and Carilli, 2019). Coral cover for all three coral morphologies (branching, massive, and *Porites rus*) calculated using the quadrat photos were highly correlated (p-values < 0.001; Figure B.1) to the coral cover calculated using the photomosaics, so statistical modelling was performed with a single metric determined from the photomosaics.

2.3 Structural complexity

2.3.1 Photographic surveys and 3D model generation

High-resolution images were captured of the reef substrate using structure from motion (SfM) photogrammetry techniques for constructing 3D models of the coral reef habitats following protocols used by Burns et al. (2015). Photos of the benthic substrate were collected over a 10 m x 10 m plot constructed in the middle of the 50 m transect along the fore reef slope (8 – 12 m depth) at each site. Diving weights were used as ground control points (GCPs) and were placed at the corners of the plot at known depths and relative spatial locations to enable accurate orthorectification of the resulting 3D reconstructions. The transect tape placed along the margin of the plot was also used to validate the spatial accuracy of the 3D models. Images of the reef substrate were collected while swimming in a lawnmower pattern approximately 2 m above the substrate (Figure 2.2). Images were taken with 70 – 80 % overlap from both planar and oblique angles. Photos were taken using a Canon PowerShot G7 X Mark II digital SLR camera with a 24 mm lens in a Fantasea FG7X II housing.

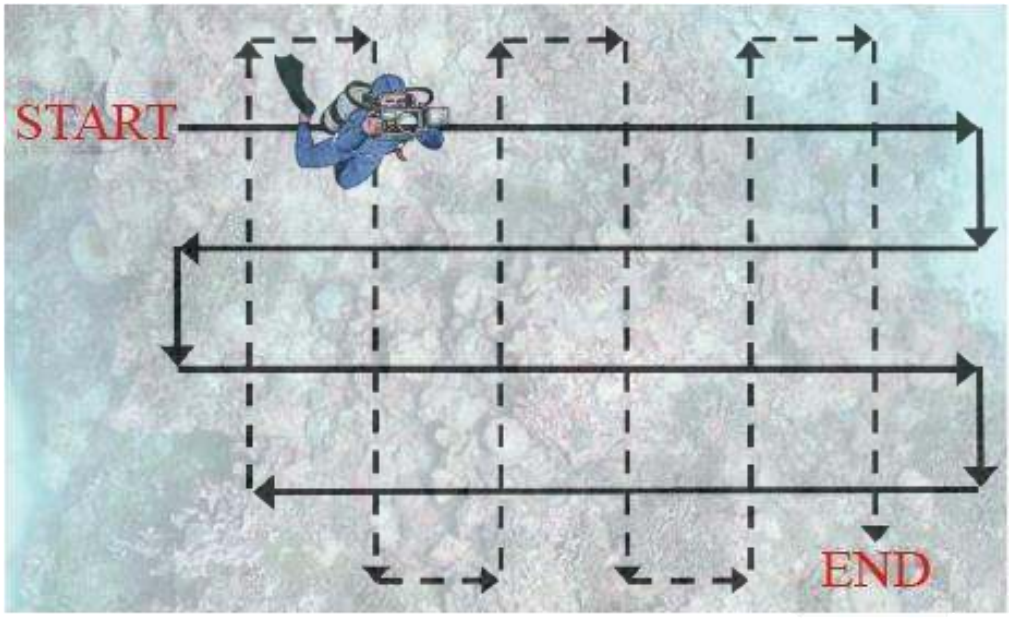

Figure 2.2 – The diver operating the camera follows this lawnmower pattern over the plot, keeping the height and orientation of the camera above the substrate consistent.

2.3.2 Quantification of structural complexity metrics

Three parameters were chosen as proxies for structural complexity: surface rugosity, standard deviation of elevation, and terrain ruggedness. These geospatial metrics were quantified using the 3D analyst and spatial analyst tools in ArcMap (version 10.6.1). The raster cells of the DEM were set to 1 cm to capture the intricate structural differences among the various morphologies of the surveyed coral colonies. Surface rugosity (or tortuosity) was quantified using the 'add surface information' tool in ArcMap to calculate the ratio of the 3D to 2D surface area for each reef plot and for all digitized polygons representing the benthic habitat. Surface rugosity is related to the traditional 'chain-and-tape' method of linear rugosity that compares the contour distance on the reef, measured by draping a chain over the benthic habitat, to a linear distance that is measured using a transect tape (Friedman et al., 2012). Surface rugosity is commonly used in studies analyzing the complexity of coral reef ecosystems (e.g., Friedman et al., 2012; Dustan et al., 2013; Burns et al., 2015; Leon et al., 2015; Magel et al., 2019; Price et al., 2019). The standard deviation of elevation (SDE; or root mean square height) describes the variability of elevation values, here defined as within a 3 x 3 cell moving window. SDE is commonly used as a parameter to measure surface roughness (Shepard et al., 2001; Lou and Kang, 2017) and is the absolute difference between the mean DEM and the DEM, divided by the range of the DEM (eq.

1). Higher values indicate areas of more pronounced vertical variations and thus more complex terrain. A study by Leon et al. (2015) used SDE as a parameter to characterize the surface roughness of Heron Reef on the southern Great Barrier Reef.

(1)

$$SDE = \frac{\sum_{n=1}^{9}(h_{mean} - h_i)}{h_{max} - h_{min}}$$

Terrain ruggedness was quantified using the 'benthic terrain modeler' tool in ArcMap which measures the 3D dispersion of vectors orthogonal to the surface of the DEM. The resultant vector ($|r|$) was calculated within a 3 x 3 cell window centered on each cell (eq. 2; where $x = \sin(\alpha) * \sin(\beta)$, $y = \sin(\alpha) * \cos(\beta)$, $z = \cos(\alpha)$, α = slope, and β = aspect). The measure of terrain ruggedness is the magnitude of the resultant vector divided by the number of cells in the neighbourhood (n), all subtracted from one (eq. 3). This method encapsulates the variability in slope and aspect into a single value. Terrain ruggedness values range from zero with no terrain variation to one with complete terrain variation (Sappington et al., 2007). Magel et al. (2019) used terrain ruggedness as a metric to calculate coral reef structural complexity across sites with varying levels of local human disturbance.

(2)

$$|r| = \sqrt{\left(\sum x\right)^2 + \left(\sum y\right)^2 + \left(\sum z\right)^2}$$

(3)

$$terrain\ ruggedness = 1 - \frac{|r|}{n}$$

2.3.3 Digital annotation of coral features

Benthic features were manually digitized on the 2D orthophotomosaic for each site using ArcMap editor tools. Unique polygon shapefiles were created for all individual living and recently dead major reef-building adult corals (≥ 5 cm diameter) and all sand patches in a smaller 8 m x 8 m plot within the larger 10 m x 10 m surveyed reef plot. A smaller plot was selected within each 3D model in order to account for variation in the size and shape of each surveyed reef plot. All three complexity metrics were calculated for the whole reef plot (i.e. 8 m x 8 m).

The orthophotomosaics were annotated to enable comparisons between the topographic complexity data for the major reef-building coral colonies (8,929 total adult coral colonies) and the sand within each surveyed substrate, following the procedure in Burns et al., 2015. The reef building coral colonies were annotated following the categories *Acropora*, *Favids*, *Heliopora*, *Pocillopora*, *Porites rus*, massive *Porites*, other branching coral, and other massive coral; the classification is based on the most common coral taxa on the Gilbert Islands reefs (Donner and Carilli, 2019). For each 8 m x 8 m plot, the coverage of each of the taxa was calculated by determining the total area occupied by each taxa and dividing by the total area of the reef plot. Also, the surface rugosity was calculated for each adult coral.

To examine the relationship between the structural complexity of different coral morphologies, each major reef-building coral was assigned to one of three growth forms (Magel et al., 2019): branching (*Acropora*, *Heliopora*, *Pocillopora*, other branching coral), massive (*Favids*, massive *Porites*, other massive coral), or *Porites rus*. *Porites rus* was assigned its own morphology category because it is very dominant in reefs around South Tarawa (Donner and Carilli, 2019) and has a distinctive morphology (encrusting with plating and branching features) in comparison to other common corals in the Gilbert Islands. The coverage and surface rugosity of each of the three morphological categories was calculated using the same methods stated above for coral taxa.

2.4 Coastal measurements

Beach surveys were conducted at all South Tarawa sites and one North Tarawa site (T05). We were unable to conduct surveys at any of the Abaiang sites or T07 since they were not adjacent to land or not accessible (i.e. no roads nearby or private property). To examine the physical factors influencing wave energy reaching the shoreline at each of the Tarawa sites, the reef flat width, surface roughness, and reef flat depth at high tide were measured at all Tarawa sites except T07, which is distant from land. The reef flat width (W) was measured using Google Earth and was calculated as the distance between the reef crest and the beach. To estimate surface roughness, during low tide we walked from the beach to the reef crest collecting photos of the reef flat. The images of the reef flat surface roughness were then used to convert the *in situ* observations into friction factor (f_w) values based on criteria outlined by Sheppard et al. (2005).

Reef flat roughness ranged from f_w = 0.08 to 0.2, where 0.08 was sand and 0.2 was rough live or dead (but not eroded) coral. The reef flat depth at high tide was estimated using standard trigonometric calculations based on visual observations of the high tide water line evidenced by the deposition of debris and algae on the beach.

2.4.1 Simple model for wave energy

The percent of offshore wave energy that reaches the shoreline behind the reef was calculated at each Tarawa site (except T07) and was estimated using a model developed by Sheppard et al. (2005). The spreadsheet-based model is based on Gourlay's (1996a, 1996b, 1997) equations of wave energy cross a reef. Sheppard et al. (2005) used the model to test the influence of reef flat width, steepness of the wave breaking zone, water level over the reef flat (i.e. simulate sea level rise), and reef flat roughness on the final wave energy reaching the shore. The input variables for the model include reef profile factor (K_p), tangent angle of the reef face or rim (tan alpha reef), offshore wave height (H_o), reef flat water depth (h_r), depth of reef edge (h_e), initial estimation of wave setup (n_r), atmospheric surge (n_w), beach slope gradient angle (tan alpha beach), reef flat width (W), increment in wave height decay (d_x), and frictional coefficient on the reef flat (f_w). The variables in the model can be changed according to measurements made for each individual reef. Average significant wave height (H_o) was set at 1.5 m, based on the value from NOAA's Wavewatch III model during the 2009 - 2010 winter where Tarawa experienced El Niño-driven high waves and shoreline damage. The h_r was set at 1.41 m based on the 2018 mean tidal range in Betio, Kiribati (Bureau of Meteorology, 2016). All reef flats were standardized with a tan alpha beach of 0.125, tan alpha reef of 0.036, and increment in wave height decay calculation of 5 based on inputs for other reef-lined shorelines (Sheppard et al., 2005). The values for W and f_w were changed according to the coastal measurements above. The reef profile factor (K_p) was estimated based on the photomosaic fore reef plot slope of each site and the corresponding K_p values outlined in Table 2 of Sheppard et al. (2005).

2.5 Statistical analyses

Statistical analyses were conducted using R version 3.5.1 (R Core Team, 2019). Information-theoretic model selection procedures were used to examine the influence of local stressors on

coral reef surface rugosity, standard deviation of elevation, and terrain ruggedness. For each structural complexity metric, linear mixed-effects (LME) models were fit with local human disturbance and the density of each of the coral morphologies used as fixed effects and atoll as a random effect (to account for non-independence among sites at the same atoll). Local human disturbance and the densities of each of the coral morphologies were modelled as continuous variables. Prior to statistical modelling, all fixed effects variables were standardized to a mean of zero and a standard deviation of one using the function 'rescale' (in package *arm;* Gelman and Yu-Sung, 2018) to allow for comparison of the effect sizes of different variables (Gelman, 2008). We also explored the possibility of including temperature variability (coefficient of variability of SST) as a fixed effect (Tables C.1 - C.3), however this was ultimately deemed to be unnecessary because of minimal variability in temperature across the sampled sites. The coefficient of variability of maximum annual SST (CV_{SST}) for each of the field sites was computed using 1985 - 2017 daily SST data from NOAA Coral Reef Watch's CoralTemp V1.0 dataset.

For each structural complexity metric, 15 models were evaluated by fitting every combination of variables. The small-sample corrected Akaike information criterion (AICc) was used to compare models and estimate the magnitude of differences between models with respect to expected predictive power. The AIC_c values were also used to produce a set of all reasonably well-fitting models that are within 10 ΔAIC_c of the best model (Bolker et al., 2008). Within the set of reasonably well fit models, model-averaged parameter estimates and 95% confidence intervals for each predictor variable were calculated in order to account for model uncertainty. The relative variable importance (RVI) of individual parameters was also determined using the function 'importance' by calculating the sum of the Akaike weights across all models containing a given parameter with the most important parameter having a maximum possible value of one. Models were fit using the R package *nlme* (Pinheiro et al., 2019) and information-theoretic model selection was performed using the package *MuMIn* (Barton, 2019).

Chapter 3: Results

This study of coral reefs in the atoll nation of Kiribati was carried out during April and May, 2018. The photomosaic data that was generated (Figure 3.1) and the reef flat observations formed the basis of the results summarized in this section. Pertinent to all analyses, the ground sample distance (resolution/pixel) for all 3D reconstructions was less than 0.01 m/pix and all the DEMs were rendered with a cell size of 1.0 cm, which is within the range of the ground sampling distance.

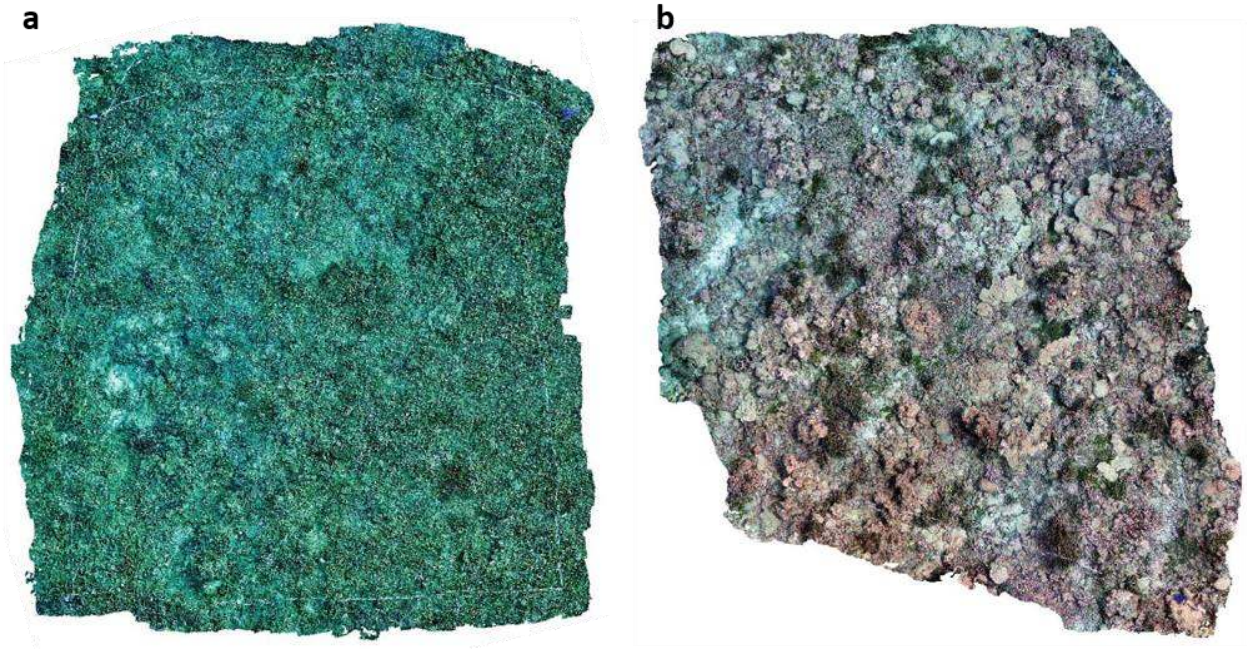

Figure 3.1 – Three-dimensional models of the benthic cover at (a) T12 in South Tarawa and (b) A03 in Abaiang.

3.1 Structural complexity across sites

A Principal Component Analysis (PCA) was used to explore the data to reveal meaningful patterns by sequentially identifying the greatest to least sources of variance in the dataset. The surface rugosity, SDE, terrain ruggedness, local human disturbance, branching coral cover, massive coral cover, *Porites rus* coral cover, average depth, slope of fore reef, and CV_{SST} were measured for all 16 sites and comprise the data used for the PCA. Table 3.1 shows the proportion of variance described by each PC and their respective Eigenvalue while the scree plot showing the proportion of variance for all 10 PCs is shown in Figure 3.2. The scree plot and the percent

cumulative variance column in Table 3.1 indicate that PC1 through PC5 explain almost 92% of the total variance in the dataset with PC1 and PC2 together contributing over two-thirds of the variance at approximately 46% and 22%, respectively. Table 3.2 shows that each PC includes positive and negative loadings. Loadings close to 1 or -1 suggest that the variable strongly influences a given PC whereas loadings approaching 0 suggest that a variable has only a weak effect on a PC. Several variables were found to influence PC1 including the coverage of corals (massive, branching, and *Porites rus*), local human disturbance, temperature variability (CV_{SST}), slope of the fore reef, and terrain ruggedness. PC2, in contrast, was dominated by two variables: surface rugosity and SDE. PC3 explained about 10% of the variance in the data and was primarily influenced by a single variable, the average depth of the site while PC4, accounting for 9.2% of the variance, was affected by several variables with coverage of branching corals the most influential amongst the top four. PC5 explained about 5% of the total variance in the dataset and was predominantly explained by CV_{SST} and to a lesser extent by the coverage of *Porites rus*. The remaining PCs together only account for about 4% of the total variance and their contributing variables are given in Table 3.2.

Table 3.1 – Summary of each Principal Component reported as a fractional proportion and cumulative contribution to total variance in the dataset and their corresponding Eigenvalues.

Principal Component	Proportion of Variance (%)	Cumulative Proportion (%)	Eigenvalue
1	45.710	45.710	2.138
2	22.090	67.800	1.486
3	9.669	77.469	0.983
4	9.207	86.676	0.960
5	5.112	91.788	0.715
6	4.369	96.156	0.661
7	2.167	98.323	0.466
8	1.038	99.361	0.322
9	0.540	99.901	0.232
10	0.099	100.000	0.100

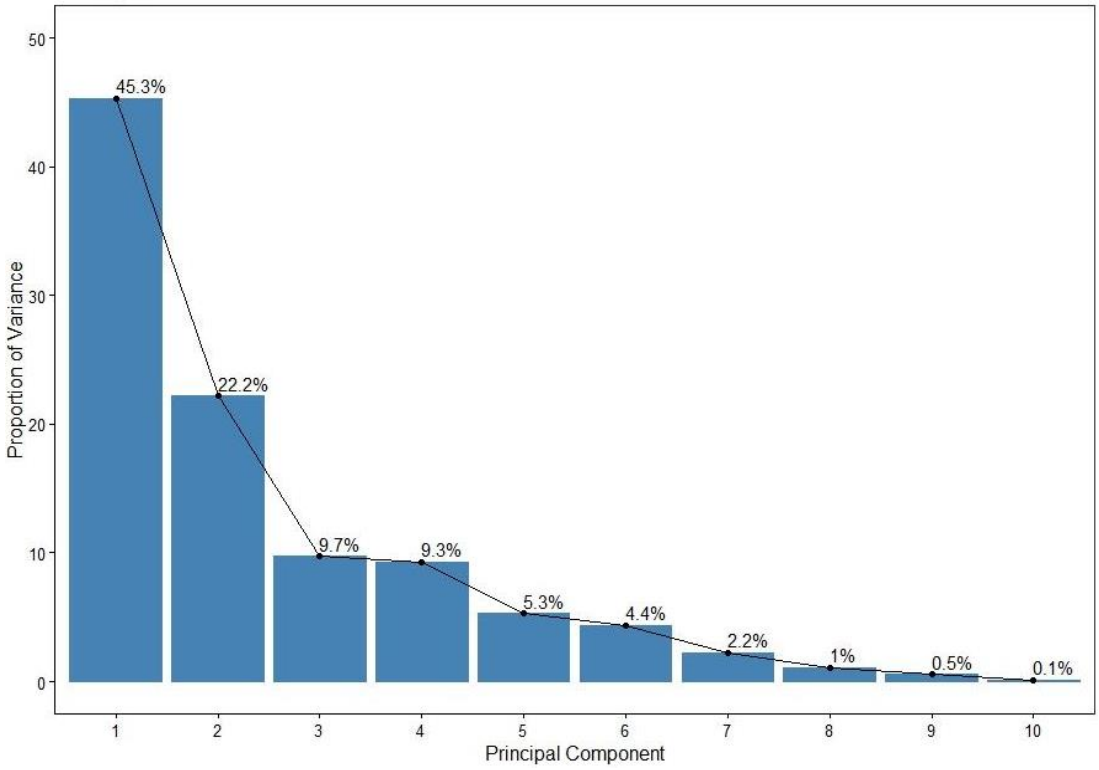

Figure 3.2 – Scree plot showing the variance for each Principal Component.

Table 3.2 – The Principal Component loading vectors for ten quantitative parameters measured over 16 sample sites with black and red depicting positive and negative values, respectively.

Parameter	PC1	PC2	PC3	PC4	PC5	PC6	PC7	PC8	PC9	PC10
1. Surface rugosity	0.034	0.649	0.017	0.218	0.055	0.032	0.194	0.056	0.294	0.631
2. SDE	0.140	0.564	0.138	0.411	0.231	0.034	0.075	0.113	0.071	0.630
3. Terrain ruggedness	0.262	0.308	0.457	0.434	0.382	0.110	0.084	0.394	0.239	0.247
4. Local human disturbance	0.412	0.078	0.032	0.045	0.317	0.215	0.793	0.069	0.083	0.185
5. Branching coral cover	0.323	0.271	0.021	0.497	0.199	0.433	0.284	0.074	0.504	0.091
6. Massive coral cover	0.431	0.032	0.044	0.314	0.035	0.118	0.116	0.527	0.580	0.264
7. *Porites rus* cover	0.407	0.189	0.018	0.020	0.455	0.129	0.018	0.630	0.395	0.148
8. Avg. depth	0.181	0.155	0.764	0.447	0.007	0.291	0.170	0.213	0.005	0.019
9. Slope of fore reef	0.357	0.107	0.326	0.086	0.001	0.795	0.002	0.130	0.308	0.063
10. CV_{SST}	0.354	0.120	0.278	0.200	0.671	0.069	0.445	0.286	0.058	0.074

A biplot of PC1 and PC2 that identifies scores for each of the 16 sampling sites near North Tarawa and South Tarawa is shown in Figure 3.3. The scores for sites in North Tarawa and Abaiang form a cluster positioned positive to the origin along PC1 while sites in South Tarawa are clustered, with one exception (T16), negative to the origin along PC1. Site T16 is geographically closest to the North Tarawa sites. Thus PC1 largely clusters sites by atoll. The parameters on the Figure 3.3 biplot show that positive influences along PC1, and hence factors that cluster scores for sites in North Tarawa, are variables related to SDE and massive and branching coral cover. In contrast, sites in South Tarawa are more strongly influenced by high

levels of human disturbance, *Porites rus*, and temperature variability as well as predominantly steeper fore reef slopes. PC2 suggests that surface rugosity and SDE are correlated variables.

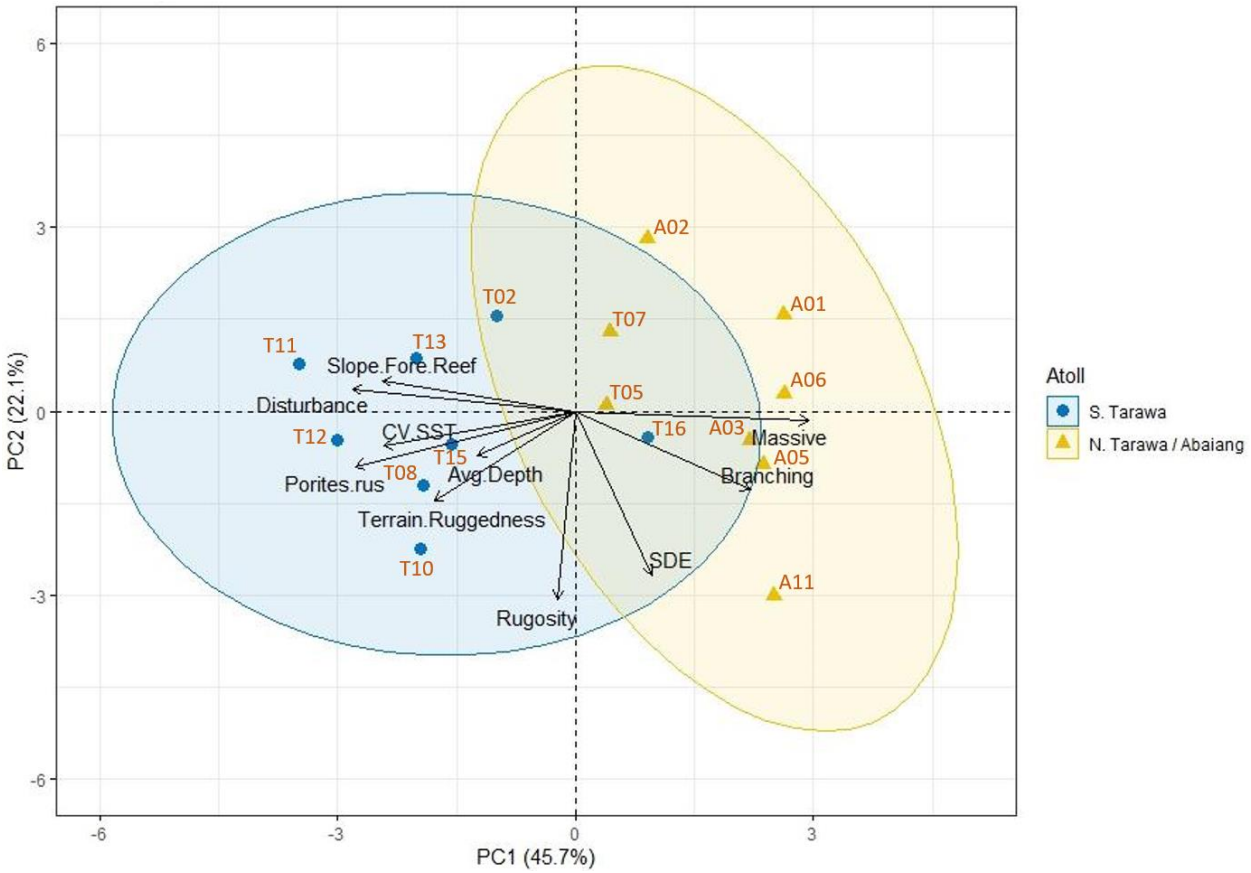

Figure 3.3 – Scores biplot for Principal Component Analysis of 10 biological and environmental parameters from 16 survey sites around Tarawa and Abaiang Atolls. Parameters along PC1 and PC2 are identified: Rugosity = surface rugosity, SDE = standard deviation of elevation, Terrain.Ruggedness = terrain ruggedness, Disturbance = local human disturbance; Branching = branching coral cover; Massive = massive coral cover; Porites.rus = *Porites rus* coral cover; Avg.Depth = average depth of the fore reef plot; Slope.Fore.Reef = slope of the fore reef plot; and CV_{SST} = coefficient of variation of maximum annual SST.

Figure 3.4 summarizes the data for the three structural complexity metrics. The average surface rugosity of the South Tarawa sites was determined to be 2.69 ± 0.35 and for North Tarawa and Abaiang sites the value was 2.52 ± 0.40 (Figure 3.4a) indicating there is no significant difference between the fore reef surface rugosity of the atolls. The average SDE of the South Tarawa sites was found to be 0.038 ± 0.006 m while the North Tarawa and Abaiang sites was 0.040 ± 0.008 m (Figure 3.4b), evidence there is no significant difference between the estimated SDE values of the atolls. Using a Pearson correlation test, the surface rugosity and SDE were found to be

significantly correlated (p-value < 0.001, Figure B.2). This correlation is reflected in the structural complexity data, with the highest, overlapping, surface rugosity value of 3.34 and highest SDE measures of 0.050 m and 0.057 m for T10 and A11 sites, respectively. Similarly, the lowest surface rugosity score at site A02, with a value of 2.02, had the second lowest SDE score of 0.03 m. Figure 3.4c provides measures of terrain ruggedness for each of the sites. The average of the South Tarawa sites for terrain ruggedness was 0.11 ± 0.02 while the corresponding average for North Tarawa and Abaiang sites was significantly lower at 0.09 ± 0.01 (p-value = 0.032, Table B.1). The range of terrain ruggedness spanned from the highest value found at site T12 (0.15) to the lowest value at site A01 (0.07).

On average, sites with a lower human disturbance metric have a lower average surface rugosity and terrain ruggedness (Table A.2). The average local human disturbance value of the South Tarawa sites was 8.02 ± 0.79 while the North Tarawa and Abaiang sites had a significantly lower (p-value < 0.001, Table B.2) average disturbance value of 4.97 ± 0.87. As such, sites that are more highly disturbed due to a large nearby village had a higher overall reef structural complexity than sites that are further from a village or area with dense population.

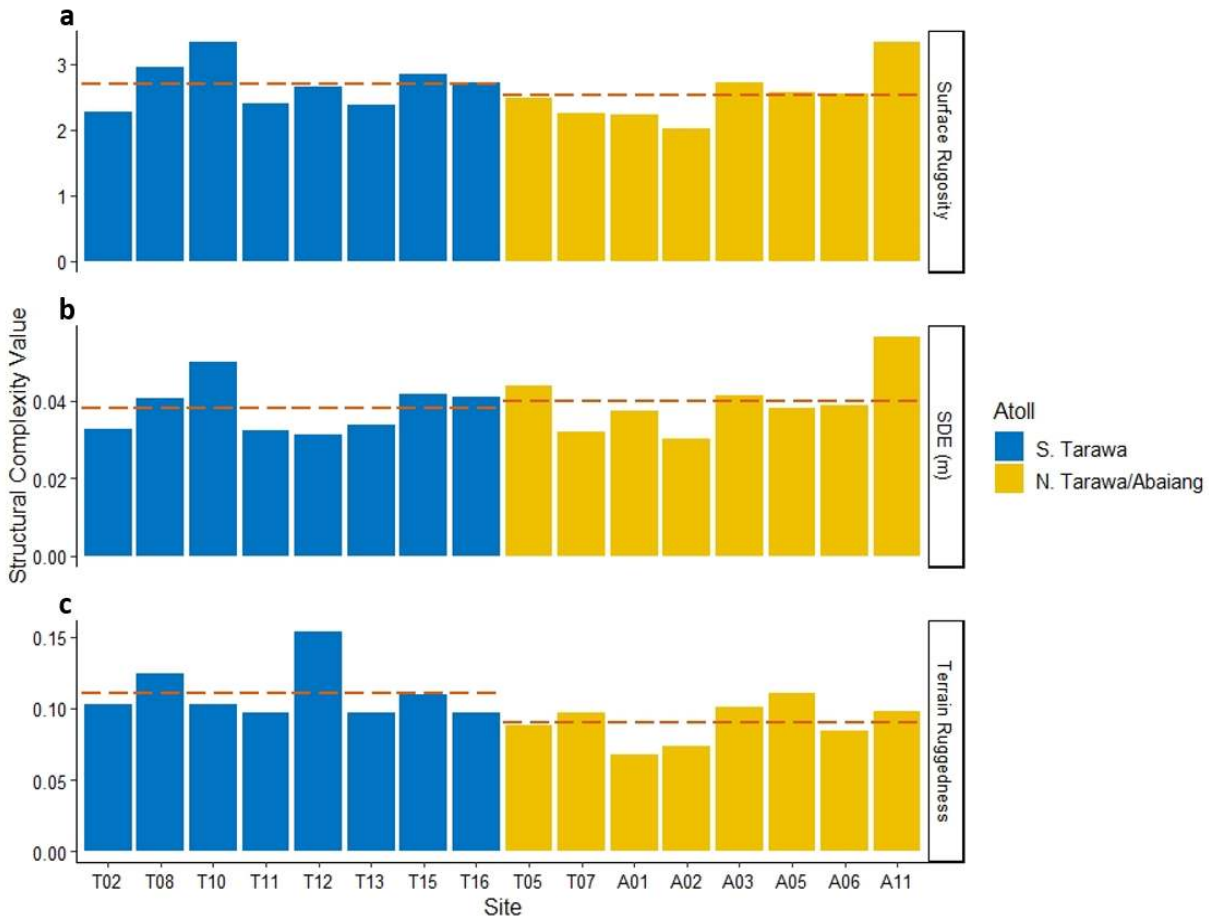

Figure 3.4 – Structural complexity characterisation of fore reef plots across 16 reef sites in Tarawa and Abaiang Atolls, Kiribati. The three complexity metrics are (a) surface rugosity, (b) standard deviation of elevation (SDE), and (c) terrain ruggedness. The orange dashed line represents the mean for each atoll. Data for each structural complexity metric can be found in Table A.3.

3.1.1 Coral taxa contribute differentially to structural complexity

The structural complexity of coral reefs is directly related to reef health, coral cover and biodiversity. Figure 3.5 offers a visual summary of benthos coverage and the reef-building corals found at the 16 sites surveyed. Dead coral and reef rock covered in algal turf were the most common benthic feature, ranging from 22% to 62% of total benthos found across all sites (Figure 3.5a). *Halimeda* spp. was the most common of the observed macroalgae at several sites, with coverage ranging from below detection (0%) up to 27% coverage. Reefs in North Tarawa and Abaiang had significantly more *Halimeda* spp. (p-value < 0.001, Table B.3). By contrast, sites in South Tarawa had significantly more cyanobacteria (p-value = 0.0029, Table B.3). In addition,

sites in South Tarawa, on average, had a higher live coral cover (34%) than sites in North Tarawa (17%).

Figure 3.5b shows that there are differences in the typical coral community compositions between sites in South Tarawa and sites in North Tarawa and Abaiang. *Porites rus* was significantly more common at sites in South Tarawa (p-value < 0.001, Table B.3) with a median of 91% coral cover. Seven of eight South Tarawa sites were dominated by *Porites rus*, the exception being site T16 where the coral cover was more biodiverse. There were no sites in South Tarawa with branching *Acropora* spp. and few with massive *Porites* and *Favids*. By contrast, sites in North Tarawa and Abaiang were dominated by *Heliopora*, *Favids* (p-value = 0.0014, Table B.3), massive *Porites*, and *Acropora*.

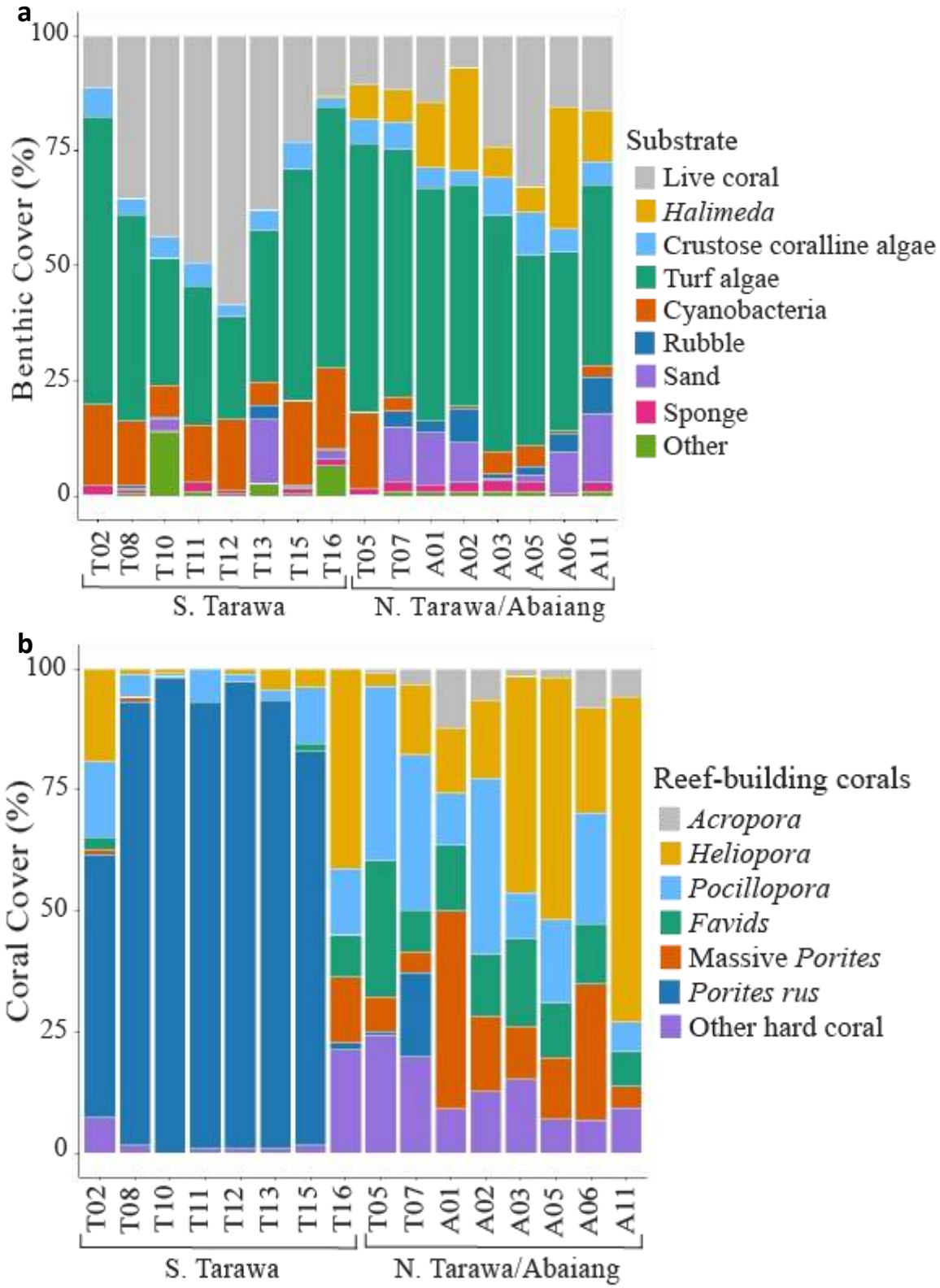

Figure 3.5 – Benthic cover of (a) key benthic categories and (b) major reef-building corals at each study site.

We examined the surface rugosity of individual features (Table A.4) to understand their relative contribution to overall structural complexity at each site. Surface rugosity of individual corals is influenced to a significant extent by coral morphology (p-value < 0.001, Table B.4). Figure 3.6 compares coral species morphology as a function of mean surface rugosity values. A Tukey HSD (Table B.5) shows that branching corals have a significantly higher mean surface rugosity relative to the massive corals (p-value < 0.001) and *Porites rus* (p-value = 0.01). Although *Porites rus* does not have as high a surface rugosity compared to branching corals (Figure 3.6), *Porites rus* contributes greatly to the overall surface rugosity of site T10 because of its high contribution to the coral cover of the fore reef at that site. In contrast, although site A02 has a higher biodiversity of corals (Figure 3.5b), the coverage of branching corals (i.e. HEL, POC) is lower compared to sites A05 and A11, with the reduced coverage resulting in a lower estimate of overall reef surface rugosity. In addition, Figure 3.6 also shows that there is no significant difference in the mean surface rugosity of the massive corals and *Porites rus*. The mean surface rugosity of each coral taxon is variable between sites, with certain taxa having high surface rugosity values (i.e. surface rugosity values > 4) at some but not all sites (Figure A.1 and Table A.4). For example, the surface rugosity of *Heliopora* is high at sites T08, T05, and A06, also true for other branching coral found at sites T08 and A11, massive *Porites* at site T10, *Pocillopora* at site T15, *Acropora* at site T05, and *Porites rus* at site A11.

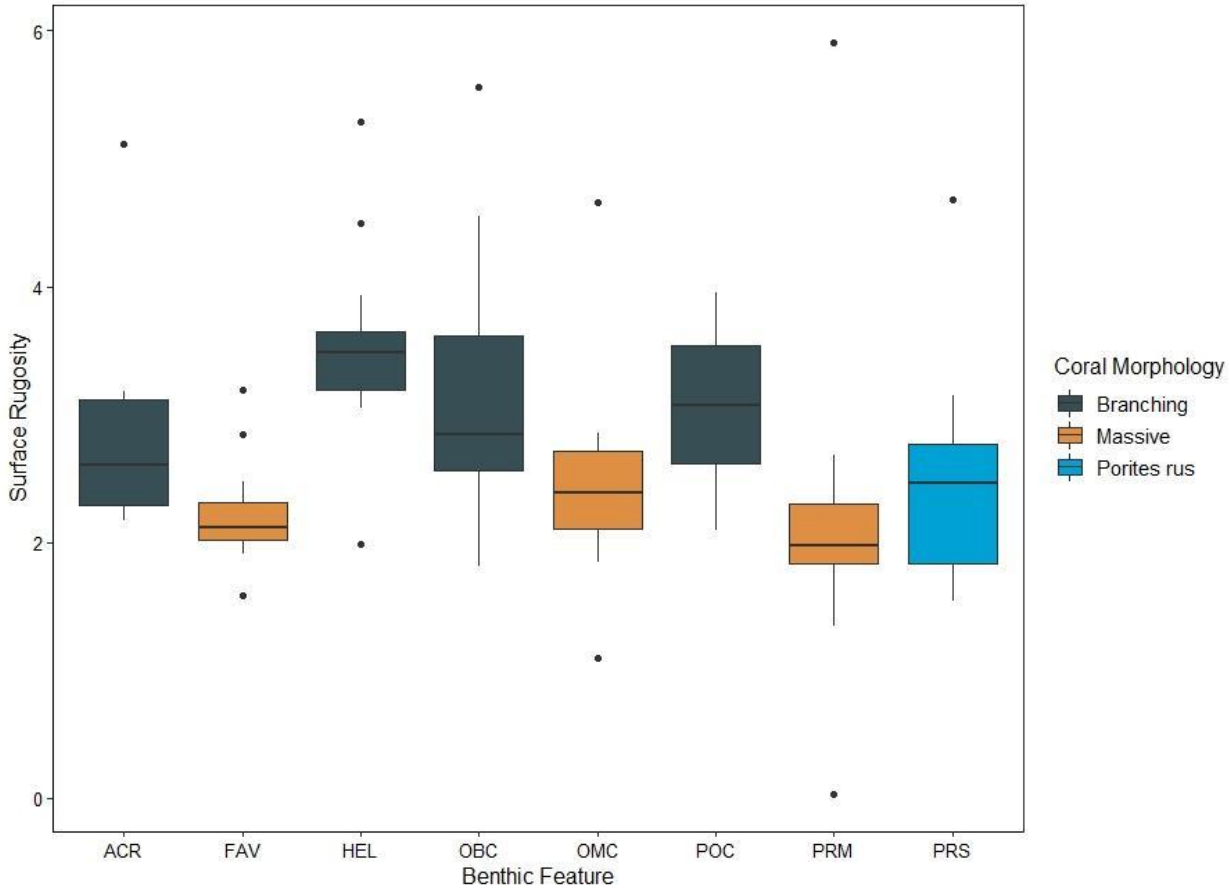

Figure 3.6 – Comparisons between the surface rugosity of key reef building coral taxa belonging to three distinct morphology classifications across all fore reef sites. ACR = *Acropora*, FAV = *Favids*, HEL = *Heliopora*, OBC = Other Branching Coral, OMC = Other Massive Coral, POC = *Pocillopora*, PRM = *Porites* Massive, PRS = *Porites rus*.

3.2 Drivers of structural complexity

Given the importance of coral reef structural complexity in protecting shorelines, understanding the drivers of reef complexity will be important in conserving reefs under future climate change scenarios. We made and tested models to describe three structural complexity metrics: surface rugosity, SDE (standard deviation of elevation), and terrain ruggedness with results, including contributing variables, summarized in Tables 3.3 - 3.5 as well as Figure 3.7. Our linear mixed-effects models indicate that reef structural complexity in Tarawa and Abaiang is predominantly determined by a combination of branching and *Porites rus* coral cover. The strongest predictors varied between surface rugosity, SDE, and terrain ruggedness, with no single predictor variable consistently explaining the reef structural complexity across all three metrics. However, branching and *Porites rus* coral cover were the strongest predictors of surface rugosity with a

relative variable importance (RVI) of 0.51 and 0.4, respectively (Table 3.3). None of the predictor variables had a strong effect on SDE, with most important parameter, branching coral, only generating an RVI of 0.29 (Table 3.4). The coverage of *Porites rus* and branching corals were the most important predictors of reef terrain ruggedness with an RVI of 0.91 and 0.55, respectively (Table 3.5). The abundance of *Porites rus* was a significant positive predictor of terrain ruggedness and sites with greater coverage of *Porites rus* (i.e. sites around South Tarawa) were associated with a higher terrain ruggedness (Figure 3.7c). The abundance of branching corals had a weak positive influence on all three structural complexity metrics as shown by the 95% confidence intervals overlapping zero (Figure 3.7). Local human disturbance and massive coral cover had very weak influences on all three structural complexity metrics, with rugosity and SDE slightly lower on reefs with a higher local disturbance value (Figure 3.7a,b). We repeated the LME analysis using additional variables CV_{SST} and average water depth of the fore reef plot and found both variables did not contribute strongly to any of three complexity metrics (Tables C.4 – C.6).

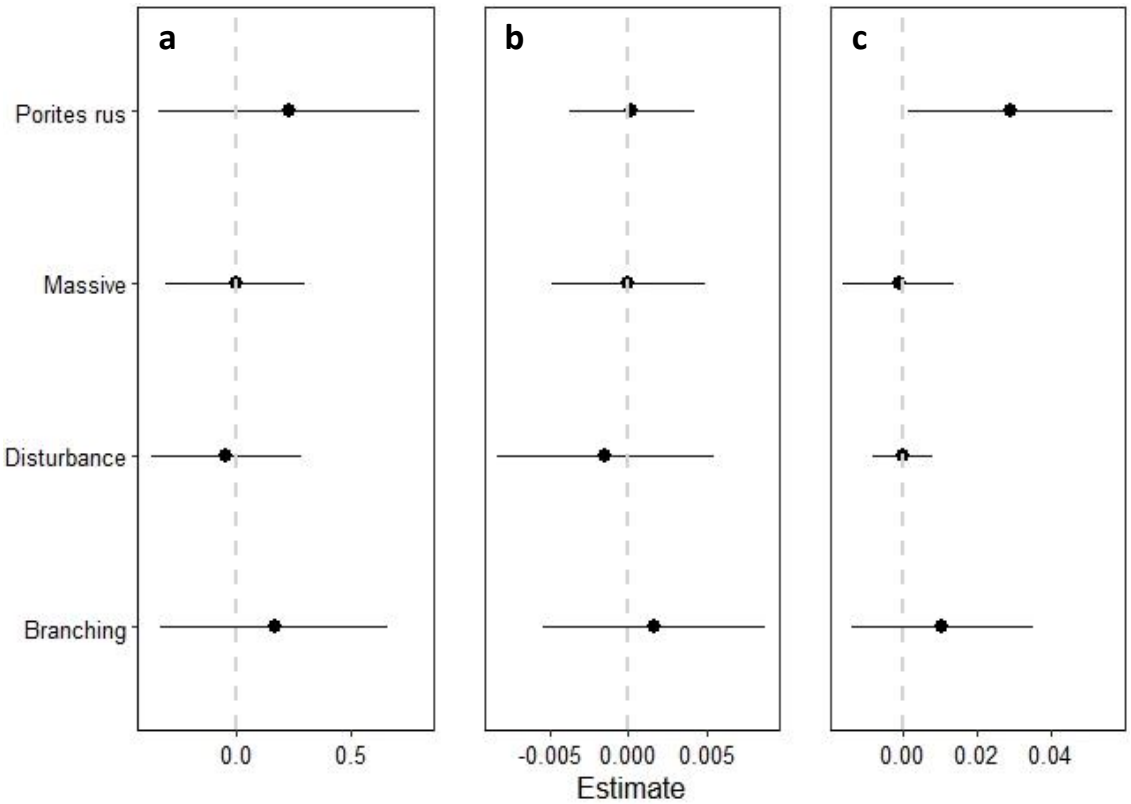

Figure 3.7 – Multi-model-averaged parameter estimates and 95% confidence intervals for predictors of (a) surface rugosity, (b) SDE, and (c) terrain ruggedness.

Table 3.3– Set of reasonably well-fitting models that describe the structural complexity metrics surface rugosity. The check marks indicate variables present within each of the models above. Disturbance = local human disturbance; Branching = branching coral cover; Massive = massive coral cover; *Porites rus* = *Porites rus* coral cover; df = degrees of freedom; AIC_c = Akaike information criteria for small sample sizes; ΔAIC_c = difference from the lowest AIC_c value (i.e. 'best' model), only models with a $\Delta AIC_c < 10$ shown; w = model weight; RVI = relative variable importance. The relative variable importance (RVI) ranges from 0 to 1, with 0 being a parameter that has no importance on the structural complexity metric and 1 being a parameter that is very important to the structural complexity metric.

Rank	Disturbance	Branching	Massive	*Porites rus*	*df*	AIC_c	ΔAIC_c	*W*
1		✓		✓	5	21.2	0.00	0.245
2				✓	4	22.4	1.24	0.132
3		✓			4	23.6	2.42	0.073
4	✓			✓	5	24.3	3.12	0.051
5			✓		4	24.5	3.27	0.048
6			✓	✓	5	25.0	3.81	0.036
7	✓				4	25.0	3.85	0.036
8		✓	✓		5	25.4	4.21	0.030
9	✓	✓		✓	6	25.7	4.46	0.026
10		✓	✓	✓	6	26.5	5.31	0.017
11	✓	✓			5	27.8	6.62	0.009
12	✓		✓		5	28.6	7.36	0.006
13	✓		✓	✓	6	29.3	8.11	0.004
14	✓	✓	✓		6	30.5	9.26	0.002
RVI	0.14	0.40	0.14	0.51				

Table 3.4 – Set of reasonably well-fitting models that describe the structural complexity metric standard deviation of elevation. See Table 3.3 for an explanation of the variables in the table.

Rank	Disturbance	Branching	Massive	*Porites rus*	*df*	AIC_c	ΔAIC_c	*W*
1		✓			4	-104.4	0.00	0.193
2	✓				4	-104.2	0.27	0.169
3			✓		4	-102.5	1.91	0.074
4				✓	4	-102.1	2.39	0.058
5	✓			✓	5	-100.7	3.72	0.030
6	✓	✓			5	-100.6	3.84	0.028
7		✓	✓		5	-100.6	3.88	0.028
8		✓		✓	5	-100.6	3.88	0.028
9	✓		✓		5	-100.2	4.23	0.023
10			✓	✓	5	-98.3	6.10	0.009
11	✓	✓	✓		6	-97.7	6.79	0.006
12	✓	✓		✓	6	-96.9	7.55	0.004
13	✓		✓	✓	6	-95.4	9.02	0.002
14		✓	✓	✓	6	-95.3	9.10	0.002
RVI	0.263	0.289	0.142	0.130				

Table 3.5 – Set of reasonably well-fitting models that describe the structural complexity metric terrain ruggedness. See Table 3.3 for an explanation of the variables in the table.

Rank	Disturbance	Branching	Massive	*Porites rus*	*df*	AIC_c	ΔAIC_c	*W*
1		✓		✓	5	-79.1	0.00	0.439
2				✓	4	-78.3	0.79	0.295
3		✓	✓	✓	6	-74.7	4.42	0.048
4			✓	✓	5	-74.5	4.62	0.044
5	✓	✓		✓	6	-74.1	5.01	0.036
6	✓			✓	5	-74.1	5.05	0.035
7			✓		4	-72.3	6.83	0.014
8	✓				4	-72.1	7.01	0.013
9		✓	✓		5	-72.1	7.05	0.013
10		✓			4	-71.7	7.42	0.011
11	✓		✓	✓	6	-69.2	9.94	0.003
RVI	0.09	0.55	0.12	0.91				

3.3 Reef flat analysis

There were no large differences between the reef flat width and water depth of the South Tarawa sites and the North Tarawa site (Table 3.6), however there was a large difference in the reef flat surface roughness. The reef flats around South Tarawa (Figure 3.8a) are predominantly smooth rock with 75% to 100% coverage by seagrass or algal turf, or sand and with less than 30% dead, but not eroded coral or boulders. By contrast, the reef flat in North Tarawa (T05) was predominantly (80%) dead intact coral or boulders greater than 30 cm, and was representative of reef flats around the north end of Tarawa (Figure 3.8b). Table 3.6 summarizes differences in the benthic composition of reef flats surrounding Tarawa, with reef flats in South Tarawa containing fewer dead coral skeletons and rubble relative to the reef flats in North Tarawa.

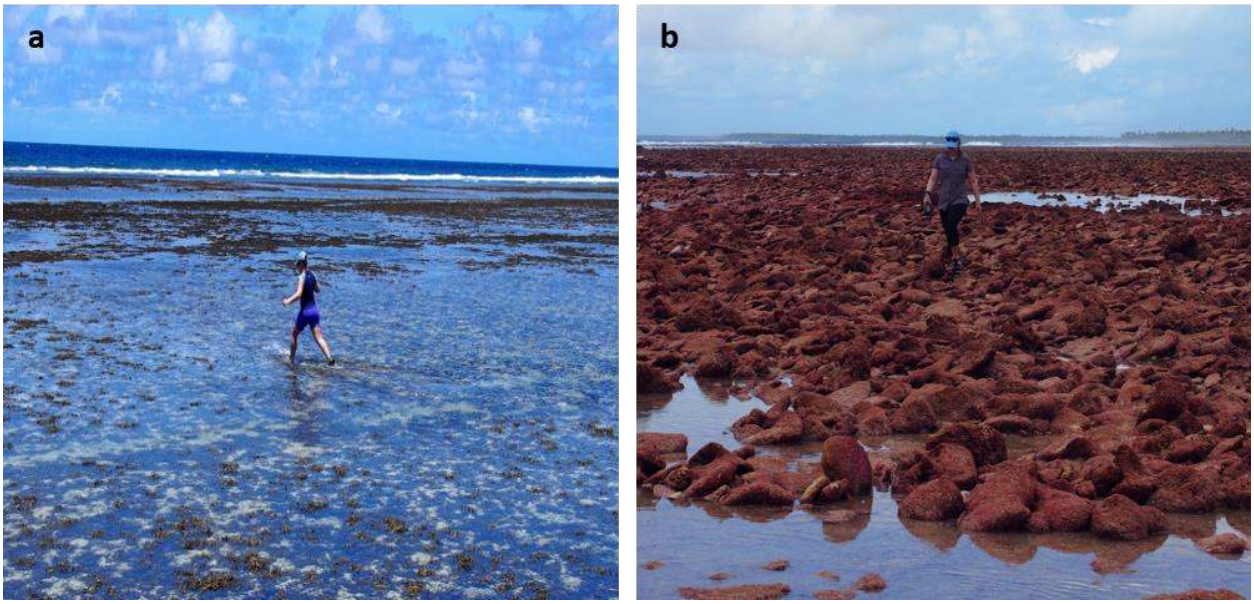

Figure 3.8 – Typical reef flat topography visible at low tide in (a) South Tarawa and (b) North Tarawa.

3.4 Wave attenuation

Based on the reef flat roughness characterisations by Sheppard et al. (2005), the wave friction factor (f_w) of reef flats in South Tarawa ranged from 0.08 at T13 to 0.14 at sites T02, T08, and T11 (Table 3.6). Reef flats in South Tarawa had an average f_w of 0.1 compared to the reef flat in North Tarawa with an f_w of 0.2. Based on the wave energy model by Sheppard et al. (2005), sites in South Tarawa had, on average, 13% of the offshore wave energy reach the shoreline behind each reef while the North Tarawa site had only 8% of the offshore wave energy reach shore

(Table 3.6). At the North Tarawa site, energy loss is up to 92% across the reef whereas the average energy loss across the South Tarawa reefs is 87%.

When sites in South Tarawa were modelled to have an f_w value similar to the North Tarawa site, the reefs were estimated to dissipate up to 93% of the offshore wave energy (Table 3.6). As such, when the South Tarawa sites increased to the friction factor approaching that of the North Tarawa site, the South Tarawa reefs would dissipate 5% more of the offshore wave energy than they do in present form. When all sites were modelled to have a reef flat f_w of 0.08 (i.e. only sand) the reefs surrounding South Tarawa and North Tarawa only dissipated 84% and 83% of the offshore wave energy, respectively (Table 3.6). Thus, when the friction factor decreases to represent a reef flat with 75 – 100% sand, reefs in South Tarawa are predicted to dissipate 4% less wave energy while the North Tarawa reefs dissipate 9% less offshore wave energy. As such, if the reef flats around North Tarawa were to be mined for infrastructure leaving only a sandy substrate, 17% of the offshore wave energy would be expected to reach the shoreline compared to the 8% at present. Overall, reef flats with a higher roughness will attenuate more offshore wave energy from reaching the shore.

When all sites were modelled to have a gentle sloping reef crest with an angle of 5 degrees (K_p = 0.47), the sites in South Tarawa and North Tarawa were predicted to dissipate 89% and 93% of the offshore wave energy, respectively (Table 3.6). As such, if erosion continues to 'round off' the reef crest, the South Tarawa and North Tarawa sites will both dissipate 1% more of the offshore wave energy than possible with a reef with a sharp reef crest. The steeper the reef crest, the higher the wave setup and therefore the higher the percentage of offshore wave energy that reaches the shoreline. In summary, the f_w of the reef flats contribute more to wave attenuation than the slope of the reef crest.

Table 3.6 – Reef flat morphology and wave energy decay due to friction for sites around Tarawa.

Site	Reef flat roughness	f_w of reef flat	Water depth at high tide m	Reef flat width m	Offshore wave energy reaching shore %	Offshore wave energy reaching shore when:		
						f_w at 0.2 %	f_w at 0.08 %	K_p at 0.47 %
T02	Smooth rock with 50% algal turf and 10% boulders	0.14	1.40	161	13.50	9.9	19.42	12.09
T08	Smooth rock with 70 – 80% algal turf and 20 – 30% boulders	0.14	1.75	211	10.83	7.58	16.67	9.65
T10	Smooth rock with 75 – 100% algal turf	0.1	2.13	221	13.81	7.21	16.19	12.38
T11	Smooth rock with 85% algal turf and 15% boulders	0.14	1.82	208	11.06	7.77	16.92	9.86
T12	Smooth rock with 70% algal turf and <10% boulders	0.12	1.40	499	<10.88	<6.41	<15.07	<9.70
T13	Smooth rock with 20% algal turf and 80% sand	0.08	1.78	649	14.54	7.77	16.92	13.04
T15	Smooth rock with 75 – 100% algal turf	0.1	1.75	210	14.54	7.77	16.92	13.04
T16	Smooth rock with 75 – 100% algal turf	0.1	2.0	381	<12.72	<6.41	<15.07	<11.38
T05	Smooth rock with 80% boulders covered in coralline algae and red algal turf and 10% sand	0.2	1.8	205	7.97	7.97	17.17	7.06

Chapter 4: Discussion

4.1 Structural complexity differs by metric and across atoll

Given the importance of healthy, structurally complex reefs in helping promote recovery post-disturbance (Graham et al., 2015) and in dissipating wave energy (Monismith et al., 2015), it is important to identify the variables driving structural complexity. We examined three different indices of coral reef structural complexity, namely surface rugosity, SDE, and terrain ruggedness. We found that the relative difference in structural complexity between the atolls depended on the index (Figure 3.4). However, surface rugosity and SDE were highly correlated and followed a similar trend across the reef plots with no significant difference in the structural complexity between the South Tarawa, and North Tarawa and Abaiang reefs (Figure 3.4a,b). In contrast, the average terrain ruggedness for the reef plots in South Tarawa were significantly higher than in North Tarawa and Abaiang (Figure 3.4c).

The abundance of certain coral growth forms is important in driving particular structural complexity metrics, thereby resulting in different general trends in complexity between the atolls. The abundance of *Porites rus* was positively related for all three structural complexity metrics (Figure 3.7), with the strongest effect for terrain ruggedness (Table 3.5). Consistent with this association, terrain ruggedness was higher in sites with greater coverage of *Porites rus*, and as such, was highest in sites around South Tarawa where *Porites rus* is dominant (Figure 3.5b). The strong positive association between *Porites rus* cover and terrain ruggedness is likely because this metric is better able to capture the fine-scale morphologies of branching and plating forms of *Porites rus*. We also found that branching coral cover had a positive impact on all three structural complexity metrics (Figure 3.7), an observation that corroborates the findings of Magel et al. (2019) and Graham and Nash (2013) who associated corals with branching traits positively to reef complexity. In contrast, we found there was a no apparent relationship between massive coral cover and reef complexity (Figure 3.7). While previous studies (Alvarez-Filip et al., 2011; Magel et al., 2019) have found a positive relationship between reef complexity and large, massive coral species, we did not find strong evidence for an interaction between massive coral cover and any of the complexity metrics we evaluated. Conceivably, the massive and submassive coral assemblages around Tarawa and Abaiang Atolls have more rounded surfaces with less fine-scale roughness relative to the massive coral species around Kiritimati, KI, that can take on

columnar or ridge-like structures (Magel et al., 2019) or the massive *Montastraea* corals around Cozumel, Mexico (Alvarez-Filip et al., 2011). Given the rounded dome structure of many massive coral genera, the contribution of massive corals to measures of reef complexity may also depend strongly on the scale at which complexity is quantified. The large-scale complexity of massive coral assemblages may not contribute as strongly as the fine-scale roughness of branching coral assemblages given the calibration scale that we used in this study.

Disturbance from bleaching events, local anthropogenic stressors, cyclones, CoT outbreaks, etc. are affecting reef complexity (Kayal et al., 2012; Burns et al., 2015; Perry and Morgan, 2017). A study conducted by Magel et al. (2019) of fore reef sites that have undergone successive heat stress events (i.e. similar to Tarawa and Abaiang Atolls) and are also exposed to a gradient of human disturbance found that reef complexity, particularly surface rugosity and terrain ruggedness, decline with increasing levels of human disturbance. Our results suggest that none of the quantified complexity metrics were substantially affected by local anthropogenic stressors (Figure 3.7 and Tables 3.3, 3.4, and 3.5). While surface rugosity and SDE were slightly lower on reefs with a higher local disturbance value (Figure 3.7a,b), the statistical relationship is weak. Both Tarawa and Abaiang have been exposed to a high frequency of bleaching-level heat stress, due to the influence of the El Niño / Southern Oscillation. The South Tarawa reefs are also exposed to high levels of local human disturbance due to stressors such as coastal infrastructure (reef rock mining to construct sea walls and the creation and maintenance of causeways), nutrient pollution (from sewage), and fishing, compared to reefs in North Tarawa and Abaiang that have very little local human disturbance (Lovell et al., 2001; Donner and Carilli, 2019). As a result, the South Tarawa reefs have favoured coral that are resilient to heat stress and anthropogenic stressors but, by consequence, the reefs have lower species evenness (Donner and Carilli, 2019). A decline in water quality and high sedimentation has led to the spread of *Porites rus,* a resilient weedy and generalist coral species (Darling et al., 2012; Padilla-Gamiño et al., 2012), at the expense of more sensitive coral species. *Porites rus* is able to able to acclimate to changes in environmental conditions on short time scales (weeks). Traits that improve the resilience of *Porites rus* to changing environmental conditions include the presence of thick tissues by allocating more energy to tissue storage than skeletal growth (i.e. calcification) during chronic stress (Padilla-Gamiño et al., 2012) and plasticity with respect to growth form by

developing either a plating or branching form under changing light levels (i.e. due to turbidity; Padilla-Gamiño et al., 2012).

Published studies reveal a tendency to interpret low coral biodiversity as an intrinsic property of low structural complexity (Chabanet et al., 1997; Bruno and Bertness, 2001). It is logical to expect that a larger variety of corals with different sizes, shapes, and forms would increase reef structural complexity and, conversely, the more homogenous a reef becomes, the more likely the reef is to have a reduced overall structural complexity. Our study of Kiribati's Gilbert Island reefs, however, finds that sites dominated by a single coral species like *Porites rus* (e.g., T12) can have higher structural complexity than more diverse reefs (Figure 3.4c). Some studies report that the distribution of species abundance (i.e. coral cover), whether by one or a few species, increases structural complexity (Alvarez-Filip et al., 2011). We found that the South Tarawa reefs are dominated by a coral species with a lower rugosity relative to other key reef building branching corals (i.e. ACR, HEL, POC; Figure 3.6) but the sites have a relatively high overall live coral cover (Figure 3.5a). The sites in North Tarawa and Abaiang, however, have a slightly higher diversity of corals, including branching corals such as *Heliopora* and *Pocillopora* that have higher rugosity (Figures 3.5a and 3.6). The coral cover of these branching corals is not high enough to increase the overall rugosity of these reefs to match the mean rugosity of South Tarawa reefs. The coral cover of many important reef-building corals is low due to past disturbances including frequent bleaching events (Donner and Carilli, 2019) and the CoT outbreak in 2013-2014 (Donner, unpublished data).

In summary, our results show that the highly disturbed sites have a more homogenized reef yet are able to maintain a higher overall structural complexity due to their higher live coral cover. Thus the generally accepted, positive association between biodiversity and structural complexity may not be universal but more context-specific. Reef complexity increases with increasing coral cover, however, the rate of increase in complexity depends, on the morphological and functional traits of the dominant coral species. As such, the type and dominance of key reef-building corals is just as important as their overall abundance in maintaining reef structural complexity (Alvarez-Filip et al., 2011).

Although the *Porites rus*-dominated reefs are able to maintain high structural complexity at present sea levels, it remains to be seen whether these corals will be able to vertically accrete fast enough to keep pace with rising sea levels (Perry and Morgan, 2017; Perry et al., 2018). If weedy corals such as *Porites rus* allocate more energy to tissue storage than skeletal growth under future environmental conditions, coral cover may be sustained but the trade-off may be a steady but less easily detected decline in vertical reef accretion. A study by Alvarez-Filip et al. (2013) found that a shift in many reef-building corals to weedy, opportunistic species resulted in losses in coral-community calcification and thus declines in reef structural complexity. As such, in addition to continuing to monitor how the structural complexity, biodiversity, and coral cover of the reefs around Tarawa and Abaiang Atolls adapt to changing environmental conditions, it would also be valuable to monitor the calcification rate of the reefs to determine whether the dominant coral species will be able to vertically accrete at a rate that keeps up with rising sea levels. Maintaining structurally complex coral communities under high sea levels in the future will reduce reef flat wave heights and swash, thereby mitigating the risk of coastal erosion (Quataert et al., 2015; Harris et al., 2018).

4.2 Coastal protection provided by reefs

Rising sea levels and wave-induced inundation threaten infrastructure and freshwater resources for atoll nations like Kiribati, conditions that have adverse consequences for the agricultural and habitation suitability of the islands (Woodroffe, 2008; Storlazzi et al., 2018). However, coral reefs are capable of helping to mitigate impacts of severe storm surges and to limit coastal erosion in low-lying atolls (Ferrario et al., 2014). The interaction between sea level, waves, and reef properties such as topography, roughness, and size govern nearshore hydrodynamics on atolls and together influence the extent to which islands are impacted by an encroaching sea.

The impact of reef flat composition on wave attenuation is greater than that of the fore reef bathymetry profile. We analyzed the reef flats of eight sites around South Tarawa and one site near North Tarawa (Table 3.6) in order to gain a better understanding of the wave energy reaching the shoreline behind reefs featuring varying levels of coral coverage and biodiversity. Using Sheppard et al.'s (2005) model of wave energy reaching reef-lined coastlines, our study considered the physical nature of reef flat width and roughness as well as the steepness of the

reef crest profile on wave attenuation. We found that the reef flat width at our sites ranged from 161 to 649 m (Table 3.6), which is similar to reef flat widths reported for other Pacific Atolls (Table 1 of Quataert et al., 2015). A meta-analysis by Ferrario et al. (2014) found that up to 50% of the reduction in wave height and energy occurs on the reef flat and within 150 m from the reef crest. Since the majority of the reef flats we analyzed were considerably wider than 150 m, we expect that increases in reef flat width will not significantly increase the frictional dissipation rates across the reefs. The steepness of the reef crest increases the wave energy reaching shore because wave energy dissipation due to wave breaking will occur along a smaller distance, thereby resulting in an increase in wave setup and ultimately an increase in wave runup. Moreover, using their model we determined that the f_w of the reef flats contribute more to wave attenuation than the slope of the reef crest (Table 3.6).

Our beach surveys indicated that the South Tarawa reef flats are dominated by smooth rock and algal turf with little to no coral rubble or boulders (Figure 3.8a) while the North Tarawa reef flat is dominated by small boulders (Figure 3.8b). It is likely that the South Tarawa reef flats once resembled the rougher reef flat in North Tarawa as a South Tarawa reef flat surveyed in 1995 consisted of coral pavement with a few boulders, and beach rock, boulders, and conglomerate at the base of the beach (Forbes and Hosoi, 1995). Ocean shoreline changes in South Tarawa are largely influenced by human activities that interfere with the natural coastal processes that would normally protect the shoreline (Biribo and Woodroffe, 2013). Even small-scale beach mining, in which shingle and coral blocks are removed for building infrastructures such as homes and seawalls, contributes to coastal erosion (Forbes and Hosoi, 1995; Lovell et al., 2001; Biribo and Woodroffe, 2013). Our results regarding offshore wave energy when f_w was 0.2 (Table 3.6) indicate that the loss of boulders on reef flats in South Tarawa have contributed towards a 5% loss in offshore wave energy dissipation, thereby increasing the threat of coastal erosion and inundation. The increase in offshore wave energy reaching shorelines (i.e. wave runup) with low bottom friction on the reef flat is in agreement with similar findings by Quataert et al. (2015) and Yao et al. (2019) who reported that a reduction in reef flat bottom roughness increased incident and infragravity wave height near the shoreline, thereby increasing wave runup.

We used the spreadsheet model proposed by Sheppard et al. (2005) for our assessment of wave energy dissipation. The advantage of using this model is that it is relatively simple compared to more complex models such as XBeach, a model requiring many hydrodynamic parameters that we were not able to accurately calculate using our available data, such as bed friction estimates. In addition, Table 1 of Sheppard et al. (2005) provides values of hydrodynamic roughness for various reef flat benthic compositions that provided us with a means of translating our *in situ* observations of the reef flats into friction factors. However, due to the simplistic nature of the model, an area for improvement would be to include parameters representing the hydrodynamically rough bathymetry of the fore reef.

Previous studies show that fore reef slope and roughness are critically important considerations in terms of wave energy dissipation across a reef (Monismith et al., 2015; Quataert et al., 2015; Harris et al., 2018; Yao et al., 2019). In a study by Quataert et al. (2015), field data and a calibrated model were used to understand the effect of different reef properties on wave-driven coastal flooding and the authors found that steep fore reef slopes (~1:10 and steeper) increased wave runup and intensified coastal erosion and flooding. In addition, a study by Monismith et al. (2015) of a healthy (i.e. nearly 100% coral cover), geometrically complex fore reef around Palmyra Atoll found that bottom friction from the complex coral canopy structure increased wave energy dissipation. The data in Figures 3.4 and 3.5, and Table A.2, show that the North and South Tarawa reefs differ with respect to fore reef slope and, depending on the structural complexity metric, can also differ in terms of bottom roughness. The steeper fore reef slopes and smoother reef flats on South Tarawa reefs relative to the North Tarawa and Abaiang reefs likely leads to higher wave energy reaching the South Tarawa shorelines, despite the higher coral cover and higher associated wave energy attenuation in South Tarawa. Clearly, more research is needed to establish whether a high coral cover, low diversity, fore reef would provide as much shoreline protection as a low coral cover, moderate diversity, fore reef.

The field of coral reef science is advancing with the emergence of SfM photogrammetry techniques for quantifying structural complexity. At the same time, advances in the use of models such as XBeach are providing simulations of complex hydrodynamics around reef shorelines. Despite these parallel advances, there is still no satisfactory method of measuring reef

roughness (i.e. structural complexity) that can be transformed into hydrodynamic parameters like f_w (Monismith, 2007; Monismith et al., 2015). As such, in the literature on coral reef roughness there is a gap between the biological and ecological *in situ* measurements of structural complexity indices (i.e. rugosity, SDE, etc.) using 3D photogrammetry and the hydrodynamic models such as XBeach that use bottom friction (f_w and c_f). Unfortunately, at present there is no accepted method for converting high resolution structural complexity measurements into friction factor values for use in hydrodynamic models.

One way to bridge the gap between the disciplines could be to do flume lab experiments such as those conducted by Yao et al. (2019) who studied the effects of various reef morphologies on incident and infragravity waves over a reef. Conceivably, 3D models generated from the SfM photogrammetry could be used to 3D-print coral reefs scaled to the wave flume to empirically test the effect of realistic fore reef morphology on wave processes over a reef. Using 3D photomosaics as templates of reefs, the wave flume would be able to determine the wave energy dissipation of naturally resilient coral systems such as those found in South Tarawa. Alternatively, in the future *in situ* studies could include pressure sensor cross-shore transects similar to the study conducted by Quataert et al., 2015 on Kwajalein Atoll, RMI. With only four pressure sensors deployed along the fore reef and outer, middle, and inner reef flat, one could monitor site-specific changes in offshore wave energy along the entire reef (Quataert et al., 2015) and not just the reef flat. From the data collected using pressure sensors one could determine the extent to which the fore reef effectively dissipates wave energy. The results would provide coastal managers with an estimate of the effect of different reef characteristics on wave-driven flooding and shoreline erosion, thus providing an indication of which shorelines may be more susceptible to the effects of climate change. In addition, since the reefs around Tarawa and Abaiang experience frequent heat stress and varying levels of human disturbance our results would provide a window into how the topography and roughness of future reefs are able to provide shoreline protection. However, given the complexity and diversity in coral reef composition and morphology (i.e. various types of reefs including fringing reefs, barrier reefs, atolls, etc.), our results may only provide hypotheses for specific reefs that resemble those around Tarawa and Abaiang. Nevertheless, with more field data on wave measurements and reef

characteristics from a variety of coral reef ecosystems, the hypotheses could be refined and extended.

Chapter 5: Conclusion

This thesis extends our understanding of the potential impacts of disturbed coral assemblages that undergo shifts in composition toward stress-tolerant, small, weedy species (i.e. *Porites rus*) on the capacity of a reef to attenuate wave energy and protect shorelines. We focused on 16 reef sites around Kiribati's Tarawa and Abaiang Atolls in order to investigate, *in situ,* the effect of differences in coral community composition on shoreline protection by comparing reef benthic cover, structural complexity and reef flat roughness. We hypothesized that the highly disturbed, *Porites rus*-dominated South Tarawa sites would exhibit a low structural complexity and display low shoreline protection as a result of the reduced wave attenuation across the reef. Through the SfM photogrammetry analysis, we found that the structural complexity of the reefs differed depending on the metric used to measure complexity. We found that the surface rugosity and SDE were not significantly different between atolls, while the average terrain ruggedness was significantly greater at the South Tarawa sites, in particular sites T12 and T08. Furthermore, through the effect size analysis, we found that the abundance of *Porites rus* and branching corals were positively related for all three complexity metrics, with the strongest positive association between *Porites rus* and terrain ruggedness. Finally, through our beach surveys we found that the South Tarawa reef flats exhibited lower benthic roughness relative to the North Tarawa site and, based on the Sheppard et al. (2005) model, would result in higher offshore wave energy reaching the shore.

In earlier studies, investigating wave dissipation across a reef has focused on collected field measurements of waves from relatively heathy reefs with high coral cover and biodiversity, and less steep reef faces (i.e. > 1:10 steepness; e.g., Monismith et al., 2015; Quataert et al., 2015). As the climate continues to warm and sea levels rise, there will be a continuing shift in coral assemblages making it important for researchers to remain vigilant in monitoring changes in fore reef structural complexity and wave attenuation, particularly for reefs that are already showing a bleaching-driven regime shift towards low coral cover and dominance of fewer and/or weedy coral species. The equatorial Gilbert Islands provide a unique opportunity to study reefs that are already undergoing more severe interannual heat stress than many other reefs around the world (Donner, 2011; Carilli et al., 2012; Karnauskas and Cohen, 2012). Although we were unable to

directly link the ecological *in situ* measurements of structural complexity indices to bottom friction parameters, future wave experiments (i.e. using pressure sensors) at the study sites we used may provide greater insights into the effects of less pristine and diverse reefs on wave attenuation.

In addition, we need more information regarding the impacts of fore reef and reef flat bottom roughness on wave attenuation to help guide community management projects to preserve shorelines that are at a higher risk of erosion and inundation. For example, increasing the vegetation fringe by planting mangroves along the coastline can help protect village infrastructures from strong ocean waves (Ellison et al., 2017). Mangroves stabilize the shorelines, improve water quality, offer a protective buffer to wind and waves, and offer a source of resources for local communities (i.e. wood and juvenile fish habitat; Ellison et al., 2017; Ellison, 2009). However, high wave energy reaching the shore can inhibit mangrove restoration. In high energy eroding coastlines in Malaysia (Hashim et al., 2010; Tamin et al., 2011) the use of applied coastal structures (e.g., gabion breakwaters, geo-textile tubes, etc.), implemented in combination with the mangrove restoration, has promoted mangrove establishment. Due to the low reef flat roughness and high population density around South Tarawa, local villages should continue planting mangroves (Baba, 2011) along the shorelines with appropriate wave energy as a cost-effective measure to protect the island from large wave events.

In closing, the results of this study suggest that under current sea level, the low diversity of coral growth forms on the fore reef in Tarawa and Abaiang will likely not affect the ability of a reef to attenuate wave energy as much as factors like coral cover, steepness of the fore reef, and composition of the reef flat. Although the coral cover, surface rugosity, and terrain ruggedness were slightly higher at most of the South Tarawa sites relative to the North Tarawa and Abaiang sites, we expect the positive influences of these parameters on shoreline protection will not outweigh the negative effects of the steep fore reef slopes and smooth reef flats around South Tarawa. With the knowledge gained by this research, an improved understanding of the reef structure around Tarawa and Abaiang is available and this can be used to inform future studies in the Pacific, as well as help to make community-managed monitoring programs more informative and effective in Kiribati.

Bibliography

Alvarez-Filip, L.,Carricart-Ganivet, J.P., Horta-Puga, G. and Iglesias-Prieto, R., 2013. Shifts in coral-assemblage composition do not ensure persistence of reef functionality. *Scientific Reports*, 3(3486). 10.1038/srep03486.

Alvarez-Filip, L., Dulvy, N.K., Côté, I.M., Watkinson, A.R. and Gill, J.A., 2011. Coral identity underpins architectural complexity on Caribbean reefs. *Ecological Applications*, 21(6), pp.2223-2231. 10.1890/10-1563.1..

Alvarez-Filip, L., Dulvy, N.K., Gill, J.A., Côté, I.M. and Watkinson, A.R., 2009. Flattening of Caribbean coral reefs: region-wide declines in architectural complexity. *Proceedings of the Royal Society B: Biological Sciences*, 276(1669). 10.1098/rspb.2009.0339.

Aung, T., Singh, A. and Prasad, U., 2009. A study of sea-level changes in the Kiribati area for the last 16 years. *Royal Meteorological Society*, 64(8). 10.1002/wea.396.

Baba, 2011. Close group planting of mangroves on atolls and coral islands of the Pacific. *ISME/GLOMIS Journal*, 9(4), pp.11-12.

Baker, A.C., Glynn, P.W. and Riegl, B., 2008. Climate change and coral reef bleaching: An ecological assessment of long-term impacts, recovery trends and future outlook. *Estuarine, Coastal and Shelf Science*, 80(4), pp.435-471. 10.1016/j.ecss.2008.09.003.

Barkley, H., Cohen, A., Golbuu, Y., Starczak, V., Decarlo, T. and Shamberger, K., 2015. Changes in coral reef communities across a natural gradient in seawater pH. *Science Advances*. 1(5), e1500328-e1500328. 10.1126/sciadv.1500328.

Barton, K., 2019. *MuMIn: Multi-Model Inference*. R package version 1.43.6. Available at: <https://CRAN.R-project.org/package=MuMIn>.

Biribo, N. and Woodroffe, C.D., 2013. Historical area and shoreline change of reef islands around Tarawa Atoll, Kiribati. *Sustainability Science*, 8, pp.345-362. 10.1007/s11625-013-0210-z.

Bolker, B.M., Brooks, M.E., Clark, C.J., Geange, S.W., Poulsen, J.R., Stevens, M.H.H. and White, J.S., 2008. Generalized linear mixed models: a practical guide for ecology and evolution. *Trends in Ecology and Evolution,* 24(3), pp.127-135. 10.1016/j.tree.2008.10.008.

Brander, R.W., Kench, P.S. and Hart, D., 2004. Spatial and temporal variations in wave characteristics across a reef platform, Warraber Island, Torres Strait, Australia. *Marine Geology*, 207(1-4), pp.169-184. 10.1016/j.margeo.2004.03.014.

Brodie, J., Fabricius, K., De'ath, G. and Okaji, K., 2005. Are increased nutrient inputs responsible for more outbreaks of crown-of-thorns starfish? An appraisal of the evidence. *Marine Pollution Bulletin*, 51(1-4), pp.266-278. 10.1016/j.marpolbul.2004.10.035.

Bruno, J.F. and Bertness, M.D., 2001. Habitat modification and facilitation in benthic marine communities. In: M.D. Bertness, S.D. Gaines, M.E. Hay, eds. *Marine Community Ecology*. Massachusetts, USA: Sinauer Associates. Ch.8, pp.201-218.

Buglass, S., Donner, S.D. and Alemu, J.I., 2016. A study on the recovery of Tobago's coral reefs following the 2010 mass bleaching event. *Marine Pollution Bulletin*, 104(1-2), pp.198-206. 10.1016/j.marpolbul.2016.01.038.

Bureau of Meteorology, 2016. *2018 Tides Tarawa (Betio), KIR*. [pdf] Australian Government. Available at: <http://www.bom.gov.au/ntc/IDO59001/IDO59001_2018_INT_TP005.pdf> [Accessed June 2019].

Burns, J.H.R., Delparte, D., Gates, R.D. and Takabayashi, M., 2015. Integrating structure-from-motion photogrammetry with geospatial software as a novel technique for quantifying 3D ecological characteristics of coral reefs. *PeerJ*, e1077. 10.7717/peerj.1077.

Cannon, S.E., Donner, S.D., Fenner, D. and Beger, M., 2019. The relationship between macroalgae taxa and human disturbance on central Pacific coral reefs. *Marine Pollution Bulletin*, 145, pp.161-173. 10.1016/j.marpolbul.2019.05.024.

Carilli, J., Donner, S.D. and Hartmann, A.C., 2012. Historical Temperature Variability Affects Coral Response to Heat Stress. *PLoS One*, 7(3), e34418. 10.1371/journal.pone.0034418.

Carilli, J. and Walsh, S., 2012. Benthic foraminifera assemblages from Kiritimati (Christmas) Island indicate human-mediated nutrification has occurred over the scale of decades. *Marine Ecology Progress Series*, 456, pp.87-99. 10.3354/meps09684.

Chabanet, P., Ralambondrainy, H., Amanieu, M. Faure, G. and Galzin, R., 1997. Relationships between coral reef substrata and fish. *Coral Reefs*, 16(2), pp.93-102. 10.1007/s003380050063.

Church, J.A., White, N.J. and Hunter, J.R., 2006. Sea-level rise at tropical Pacific and Indian Ocean islands. *Global and Planetary Change*, 53(3), pp.155-168. 10.1016/j.gloplacha.2006.04.001.

Costa, M.B.S.F, Araújo, M., Araújo, T.C.M. and Siegle, E., 2016. Influence of reef geometry on wave attenuation on a Brazilian coral reef. *Geomorphology*, 253, pp.318-327. 10.1016/j.geomorph.2015.11.001.

Crook, E.D., Cohen, A.L., Rebolledo-Vieyra, M., Hernandez, L. and Paytan, A., 2013. Reduced calcification and lack of acclimatization by coral colonies growing in areas of persistent natural acidification. *Proceedings of the National Academy of Sciences of the United States of America*, 110(27), 11044-9. 10.1073/pnas.1301589110.

Darling, E.S., Alvarez-Filip, L., Oliver, T.A., McClanahan, T.R. and Côté, I.M., 2012. Evaluating life-history strategies of reef corals from species traits. *Ecology Letters*, 15, pp.1378-1386. 10.1111/j.1461-0248.2012.01861.x.

Darling, E.S., Graham, N.A.J., Januchowski-Hartley, F.A., Nash, K.L., Pratchett, M.S. and Wilson, S.K., 2017. Relationships between structural complexity, coral traits, and reef fish assemblages. *Coral Reefs*, 36, pp.561-575. 10.1007/s00338-017-1539-z.

Donner, S.D., 2011. An evaluation of the effect of recent temperature variability on the prediction of coral bleaching events. *Ecological Applications*, 21(5), pp.1718-1730. 10.1890/10-0107.1

Donner, S.D. and Carilli, J., 2019. Resilience of Central Pacific reefs subject to frequent heat stress and human disturbance. *Scientific Reports*, 9(3484). 10.1038/s41598-019-40150-3.

Donner, S.D., Kirata, T. and Vieux, C., 2010. Recovery from the 2004 coral bleaching event in the Gilbert Islands, Kiribati. *Atoll Research Bulletin*, 587, pp.1-25. 10.5479/si.00775630.587.

Dustan, P., Doherty, O. and Pardede, S., 2013. Digital Reef Rugosity Estimates Coral Reef Habitat Complexity. *PLoS ONE*, 8(2), e57386. 10.1371/journal.pone.0057386.

Duvat, V.K.E., 2019. A global assessment of atoll island planform changes over the past decades. *WIREs Climate Change*, 10, e557. 10.1002/wcc.557.

Ellison, J.C., 2009. Wetlands of the Pacific Island region. *Wetlands Ecology and Management*, 17(3), pp.169-206. 10.1007/s11273-008-9097-3.

Elliff, C.I. and Silva, I.R., 2017. Coral reefs as the first line of defense: Shoreline protection in face of climate change. *Marine Environmental Research*, 127, pp.148-154. 10.1016/j.marenvres.

Enochs, I., Manzello, D., Kolodziej, G., Noonan, S., Valentino, L. and Fabricius, K., 2016. Enhanced macroboring and depressed calcification drive net dissolution at high-CO_2 coral reefs. *Proceedings of the Royal Society B: Biological Sciences*, 283(1842). 10.1098/rspb.2016.1742.

Fabricius, K., Langdon, C., Uthicke, S., Humphrey, C., Noonan, S., De'ath, G., Okazaki, R., Muehllehner, N., Gutbrod, M. and Lough, J., 2011. Losers and winners in coral reefs acclimatized to elevated carbon dioxide concentrations. *Nature Reports Climate Change*. 1(3), pp.165-169. 10.1038/nclimate1122.

Ferrario, F., Beck, M.W., Storlazzi, C.D., Micheli, F., Shepard, C.C. and Airoldi, L., 2014. The effectiveness of coral reefs for coastal hazard risk reduction and adaptation. *Nature Communications*, 5(3794). 10.1038/ncomms4794.

Forbes, D.I. and Hosoi, Y., 1995. Coastal Erosion in South Tarawa, Kiribati. *SOPAC Technical Report*, 255, pp.1-91.

Friedman, A., Pizarro, O., Williams, S.B., Johnson-Roberson, M., 2012. Multi-Scale Measures of Rugosity, Slope and Aspect from Benthic Stereo Image Reconstructions. *PLoS ONE*, 7(12), e50440. 10.1371/journal.pone.0050440.

Gelman, A., 2008. Scaling regression inputs by dividing by two standard deviations. *Statistics in Medicine*, 27(15), pp. 2865-2873. 10.1002/sim.3107.

Gelman, A. and Yu-Sung, S., 2018. *arm: Data Analysis Using Regression and Multilevel/Hierarchical Models*. R package version 1.10-1. Available at: < https://CRAN.R-project.org/package=arm>.

Gourlay, M.R., 1996a. Wave set-up on coral reefs. 1. Set-up and wave-generated flow on an idealised two dimensional horizontal reef. *Coastal Engineering*, 27(3-4), pp.161-193. 10.1016/0378-3839(96)00008-7.

Gourlay, M.R., 1996b. Wave set-up on coral reefs. 2. set-up on reefs with various profiles. *Coastal Engineering*, 28(1-4), pp.17-55. 10.1016/0378-3839(96)00009-9.

Gourlay, M.R., 1997. Wave set-up on coral reefs: Some practical applications. In: *Proceedings 13th Australasian Coastal and Ocean Engineering Conference and 6th Australasian Port and Harbour Conference.* Christchurch, N. Z., 1997. Vol. 2, pp. 959-964.

Gourlay, M.R. and Colleter, G., 2005. Wave-generated flow on coral reefs – an analysis for two-dimensional horizontal reef-tops with steep faces. *Coastal Engineering*, 52(4), pp.353387. 10.1016/j.coastaleng.2004.11.007.

Graham, N.A.J., Jennings, S., MacNeil, A., Mouillot, D. and Wilson, S.K., 2015. Predicting climate-driven regime shifts versus rebound potential in coral reefs. *Nature*, 518, pp. 94-97. 10.1038/nature14140.

Graham, N.A.J. and Nash, K.L., 2013. The importance of structural complexity in coral reef ecosystems. *Coral Reefs*, 32, pp.315-325. 10.1007/s00338-012-0984-y.

Guest, J.R., Low, J., Tun, K., Wilson, B., Ng, C., Raingeard, D., Ulstrup, K.E., Tanzil, J.T.I., Todd, P.A., Toh, T.C., McDougald, D., Chou, L.M., Steinberg, P.D., 2016. Coral community response to bleaching on a highly disturbed reef. *Scientific Reports*, 6, 20717. 10.1038/srep20717.

Harris, D.L., Rovere, A., Casella, E., Power, H., Canavesio, R., Collin, A., Pomeroy, A., Webster, J.M. and Parravicini., 2018. Coral reef structural complexity provides important coastal protection from waves under rising sea levels. *Science Advances*, 4(2), 10.1126/sciadv.aao4350.

Hashim, R., Kamali, B., Tamin, N.M. and Zakaria, R., 2010. An integrated approach to coastal rehabilitation: Mangrove restoration in Sungai Haji Dorani, Malaysia. *Estuarine, Coastal and Shelf Science*, 86(1), pp.118-124. 10.1016/j.ecss.2009.10.021.

Heron, S.F., Maynard, J.A., van Hooidonk, R., Eakin, C.M., 2016. Warming Trends and Bleaching Stress of the World's Coral Reefs 1985-2012. *Scientific Reports*, 6, 38402. 10.1038/srep38402.

Hoegh-Guldberg, O., 1999. Climate Change, Coral Bleaching and the Future of the World's Coral Reefs. *Marine and Freshwater Research*, 50(8), pp.839-866. 10.1071/MF99078.

Hoegh-Guldberg, O., Mumby, P.J., Hooten, A.J., Steneck, R.S., Greenfield, P., Gomez, E., Harvell, C.D., Sale, P.F., Edwards, A.J., Caldeira, K., Knowlton, N., Eakin, C.M., Iglesias-Prieto, R., Muthiga, N., Bradbury, R.H., Dubi, A. and Hatziolos, M.E., 2007. Coral Reefs Under Rapid Climate Change and Ocean Acidification. *Science*, 318(5857), pp.1737-1742. 10.1126/science.1152509.

Hughes, T., Kerry, J., Álvarez-Noriega, M. *et al*., 2017. Global warming and recurrent mass bleaching of corals. *Nature*, 543, pp.373–377. 10.1038/nature21707.

Jago, O.K., Kench, P.S. and Brander, R.W., 2007. Field observations of wave-driven water-level gradients across a coral reef flat. *Journal of Geophysical Research*, 112(C06027), pp.114. 10.1029/2006JC003740.

Karnauskas, K.B. and Cohen, A.L., 2012. Equatorial refuge amid tropical warming. *Nature Climate Change*, 2, pp.530-534. 10.1038/nclimate1499.

Kayal, M., Vercelloni, J., de Loma, T.L., Bosserelle, P., Chancerelle, Y., Geoffroy, S., Stievenart, C., Michonneau, F., Penin, L., Planes, S. and Adjeroud, M., 2012. Predator Crown-of-Thorns Starfish (*Acanthaster planci*) Outbreak, Mass Mortality of Corals, and Cascading Effects on Reef Fish and Benthic Communities. *PLoS ONE*, 7(10), e47363. 10.1371/journal.pone.0047363.

Kench, P.S. and Brander, R.W., 2006. Wave Processes on Coral Reef Flats: Implications for Reef Geomorphology Using Australian Case Studies. *Journal of Coastal Research*, 221, pp.209–223. 10.2112/05A-0016.1

Kench, P.S. and Cowell, P.J., 2001. The Morphological Response of Atoll Islands to Sea-Level Rise. Part 2: Application of the Modified Shoreface Translation Model (STM*). Journal of Coastal Research*, 34, pp.645-656.

Kench, P.S. Ford, M.R. and Owen, S.D., 2018. Patterns if island change and persistence offer alternate adaptation pathways for atoll nations. *Nature Communications*, 9, 605. 10.1038/s41467-018-02954-1.

Kohler, K.E. and Gill, S.M., 2006. Coral point count with excel extensions (CPCe): a visual basic program for the determination of coral and substrate coverage using random point count methodology. *Computers & Geosciences*, 32(9), pp.1259-1269. 10.1016/j.cageo.2005.11.009.

Kroeker, K.J., Reguero, B.G., Rittelmeyer, P. and Beck, M.W., 2016. Ecosystem Service and Coastal Engineering Tools for Coastal Protection and Risk Reduction In: Managing coasts with natural solutions: Guidelines for measuring and valuing the coastal protection services of mangroves and coral reefs. In: Beck, M.W. and Lange, G-M., eds. 2016. *WAVES*. World Bank. Ch.4, pp. 54-67.

Leon, J.X., Roelfsema, C.M., Saunders, M.I. and Phinn, S.R., 2015. Measuring coral reef terrain roughness using 'Structure-from-Motion' close-range photogrammetry. *Geomorphology*, 242, pp.21-28. 10.1016/j.geomorph.2015.01.030.

Lou, Y. and Kang, Z., 2017. Comparative study of lunar roughness from multi-source data. In: *International Symposium on Planetary Remote Sensing and Mapping*. Hong Kong, 13-16 August 2017. The International Archives of the Photogrammetry, Remote Sensing and Spatial Information Sciences, Volume XLII-3/W1.

Lovell, E., 2000. Coral reef benthic surveys of Tarawa and Abaiang Atolls, Republic of Kiribati. SOPAC Technical Report 310.

Lovell, E.R., Kirata, T. and Tekinaiti, T., 2001. *Status report for Kiribati's coral reefs*. [pdf] Available at: http://horizon.documentation.ird.fr/exl-doc/pleins_textes/divers14-11/010032214.pdf [Accessed June 2019].

Lowe, R.J., Falter, J.L., Bandet, M.D., Pawlak, G., Atkinson, M.J., Monismith, S.G. and Koseff, J.R., 2005. Spectral wave dissipation over a barrier reef. *Journal of Geophysical Research*, 110(C04001). 10.1029/2004JC002711.

Madin J.S., Hughes T.P. and Connolly S.R., 2012. Calcification, storm damage and population resilience of tabular corals under climate change. *PLoS One*, 7(10), e46637. 10.1371/journal.pone.0046637.

Magel, J.M.T., Burns, J.H.R., Gates, R.D. and Baum, J.K., 2019. Effects of bleaching-associated mass coral mortality on reef structural complexity across a gradient of local human disturbance. *Scientific Reports*, 9(2512). 10.1038/s41598-018-37713-1.

Massel, S.R. and Gourlay, M.R., 2000. On the modelling of wave breaking and set-up on coral reefs. *Coastal Engineering*, 39(1), pp.1-27. 10.1016/S0378-3839(99)00052-6.

Ministry of Finance and Economic Development, 2016. *2015 Population and Housing Census*. [pdf] Tarawa: National Statistics Office. Available at: < http://www.mfed.gov.ki/statistics/documents/2015_Population_Census_Report_Volume_1final_211016.pdf>.

Mollica, N.R., Guo, W., Cohen, A.L., Huang, K-F., Foster, G.L., Donald, H.K. and Solow, A.R., 2018. Ocean acidification affects coral growth by reducing skeletal density. *PNAS*, 115(8), pp.1754-1759. 10.1073/pnas.1712806115.

Monismith, S.G., 2007. Hydrodynamics of Coral Reefs. *Annual Review of Fluid Mechanics*, 39, pp.37-55. 10.1146/annurev.fluid.38.050304.092125.

Monismith, S.G., Rogers, J.S., Koweek, D. and Dunbar, R.B., 2015. Frictional wave dissipation on a remarkably rough reef. *Geophysical Research Letters*, 42, pp.4063-4071. 10.1002/2015GL063804.

Nelson, R.C., 1996. Hydraulic roughness of coral reef platforms. *Applied Ocean Research*, 18(5), pp.265-274. 10.1016/S0141-1187(97)00006-0.

Nyström, M., Folke, C. and Moberg, F., 2000. Coral reef disturbance and resilience in a human-dominated environment. *Trends in Ecology and Evolution*, 15, pp. 413–417. 10.1016/ S0169-5347(00)01948-0.

Osorio-Cano, J.D., Osorio, A.F. and Peláez-Zapata, D.S., 2017. Ecosystem management tools to study natural habitats as wave damping structures and coastal protection mechanisms. *Ecological Engineering*. 10.1016/j.ecoleng.2017.07.015.

Padilla-Gamiño, J.L., Hanson, K.M., Stat, M. and Gates, R.D., 2012. Phenotypic plasticity of the coral *Porites rus*: Acclimatization responses to a turbid environment. *Journal of Experimental Marine Biology and Ecology*, 434-435, pp.71-80. 10.1016/j.jembe.2012.08.006.

Perry, C.T., Alvarez-Filip, L., Graham, N., Mumby, P.J., Wilson, S.K., Kench, P.S., Manzello, D.P., Morgan, K.M., Slangen, A.B.A., Thompson, D.P., Januchowski-Hartley, F., Smithers, S.G., Steneck, R.S., Carlton, R., Edinger, E.N., Enochs, I.C., Estrada-Saldívar, N., Haywood, M.D.E., Kolodziej, G., Murphy, G.N., Pérez-Cervantes, E., Suchley, A., Vanlentino, L., Boenish, R., Wilson, M. and Macdonald, C., 2018. Loss of coral reef growth capacity to track future increases in sea level. *Nature*, 558(7710), pp.396-400. 10.1038/s41586-018-0194-z.

Perry, C.T., Alvarez-Filip, L., Graham, N.A.J., Mumby, P.J., Wilson, S.K., Kench, P.S., Manzello, D.P., Morgan, K.M., Slangen, A.B.A., Thomson, D.P., Januchowski-hartley, F., Smithers, S.G., Steneck, R.S., Carlton, R., Edinger, E.N., Enochs, I.C., Estrada-Saldivar, N., Haywood, M.D.E., Kolodziej, G., Murphy, G.N., Perez-Cervantes, E., Suchley, A., Valentino,

L., Boenish, R., Wilson, M. and Macdonald, C., 2018. Loss of coral reef growth capacity to track future increases in sea level. *Nature*, 558, pp.396–400. 10.1038/s41586-018-0194-z.

Perry, C.T. and Morgan, K.M., 2017. Bleaching drives collapse in reef carbonate budgets and reef growth potential on southern Maldives reefs. *Scientific Reports*, 7(40581). 10.1038/srep40581.

Pinheiro, J., Bates, D., DebRoy, S., Sarkar, D. and R Core Team, 2019. *nlme: Linear and Nonlinear Mixed Effects Models*. R package version 3.1-140. Available at: <https://CRAN.R-project.org/package=nlme>.

Price, D.M., Robert, K., Callaway, A., Lo lacono, C., Hall, R.A. and Huvenne, V.A.I., 2019. Using 3D photogrammetry from ROV video to quantify cold-water coral reef structural complexity and investigate its influence on biodiversity and community assemblage. *Coral Reefs,* 38(5), pp.1007-1021. 10.1007/s00338-019-01827-3.

Principe, P., Bradley, P., Yee, S., Fisher, W., Johnson, E., Allen, P. and Campbell, D., 2012. *Quantifying Coral Reef Ecosystem Services*. [pdf] Research Triangle Park, NC: U.S. Environmental Protection Agency.

Quataert, E., Storlazzi, C., van Rooijen, A., Cheriton, C. and van Dongeren, A., 2015. The influence of coral reefs and climate change on wave-driven flooding of tropical coastlines. *Geophysical Research Letters*, 42, pp. 5407-6415. 10.1002/2015GL064861.

R Core Team, 2019. *R: A language and environment for statistical computing* (version 3.5.1). [computer program] Vienna: R Foundation for Statistical Computing. Available at: <https://www.R-project.org/>.

Rogers, J.S., Monismith, S.G., Koweek, D.A. and Dunbar, R.B., 2016. Wave dynamics of a Pacific Atoll with high frictional effects. *Journal of Geophysical Research: Oceans*, 121(1), pp.350–367. 10.1002/2015JC011170.

Sammarco P.W. and Risk M.J., 1990. Large-scale patterns in internal bioerosion of *Porites*: Cross continental shelf trends on the Great Barrier Reef. *Marine Ecology Progress Series*, 59, pp.145–156. 10.3354/meps059145.

Sappington, J.M., Longshore, K.M. and Thompson, D.B., 2007. Quantifying Landscape Ruggedness for Animal Habitat Analysis: A Case Study Using Bighorn Sheep in the Mojave Desert. *The Journal of Wildlife Management*, 71(5), pp.1419-1426. 10.2193/2005-723.

Saunders, M.I., Albert, S. Roelfsema, C., Leon, J.X., Woodroffe, C.D., Phinn, S. and Mumby, P., 2015. Tectonic subsidence provides insight into possible coral reef futures under rapid sea-level rise. *Coral Reefs*, 35(1), pp.155-167. 10.1007/s00338-015-1365-0.

Schoepf, V., Grottoli, A.G., Levas, S.J., Aschaffenburg, M.D., Baumann, J.H., Matsui, Y. and Warner, M.E., 2015. Annual coral bleaching and the long-term recovery capacity of coral. *Proceedings of the Royal Society of London B: Biological Sciences*, 282(1819). 10.1098/rspb.2015.1887.

Schönberg, C.H.L., Fang, J.K.H., Carreiro-Silva, M., Tribollet, A. and Wisshak, M., 2017. Bioerosion: the other ocean acidification problem. *ICES Journal of Marine Science*, 74, pp.895-925. 10.1093/icesjms/fsw254.

Shepard, M.K., Campbell, B.A., Bulmer, M.H., Farr, T.G., Gaddis, L.R. and Plaut, J.J., 2001. The roughness of natural terrain: A planetary and remote sensing perspective. *Journal of Geophysical Research*, 106(E12), pp.32777-32795. 10.1016/j.ecss2005.02.016.

Sheppard, C., Dixon, D.J., Gourlay, M., Sheppard, A., Payet, R., 2005. Coral mortality increases wave energy reaching shores protected by reef flats: Example from the Seychelles. *Estuarine, Coastal and Shelf Science*, 64, pp.223-234. 10.1016/j.ecss.2005.02.016.

Solomon, S.M., and Forbes, D.L., 1999. Coastal hazards and associated management issues on South Pacific Islands. *Oceans and Coastal Management*, 42, pp.523-554. 10.1016/S0964-5691(99)00029-0.

Spalding, M.D., Ruffo, S., Lacambra, C., Meliane, I., Hale, L.Z., Shepard, C.C. and Beck, M.W., 2014. The role of ecosystems in coastal protection: Adapting to climate change and coastal hazards. *Ocean and Coastal Management*, 90, pp.50–57. 10.1016/j.ocecoaman.2013.09.2007.

Storlazzi, C.D., Gingerich, S.B., van Dongeren, A., Cheriton, O.M., Swarzenski, P.W., Quataert, E., Voss, C.I., Field, D.W., Annamalai, H., Piniak, G.A. and McCall, R., 2018. Most atolls will be uninhabitable by the mid-21st century because of sea-level rise exacerbating wave-driven flooding. *Science Advances*, 4(4), eaap9741. 10.1126/sciadv.aap9741.

Tamin, N.M., Zakaria, R., Hashim, R. and Yin, Y., 2011. Establishment of *Avicennia marina* mangroves on accreting coastline at Sungai Haji Dorani, Selangor, Malaysia. *Estuarine, Coastal and Shelf Science*, 94(4), pp.334-342. 10.1016/j.ecss.2011.07.009.

van Woesik, R., Sakai, K., Ganase, A. and Loya, Y., 2011. Revisiting the winners and the losers a decade after coral bleaching. *Marine Ecology Progress Series*, 434, pp.67-76. 10.3354/meps09203.

van Woesik R., van Woesik K., van Woesik L., van Woesik S., 2013. Effects of ocean acidification on the dissolution rates of reef-coral skeletons. *PeerJ*, 1, e208. 10.7717/peerj.208.

Vernon, J., Stafford-Smith, M., DeVantier, L. and Turak, E., 2015. Overview of distribution patterns of zooxanthellate Scleractinia. *Frontiers in Marine Science*, 1(81). 10.3389/fmars.2014.00081.

Webb, A.P. and Kench, P.S., 2010. The dynamic response of reef islands to sea-level rise: Evidence from multi-decadal analysis of island change in the Central Pacific. *Global and Planetary Change,* 72(3), pp.234–246. 10.1016/j.gloplacha.2010.05.003.

Weber, M., de Beer, D., Lott, C., Polerecky, L., Kohls, K., Abed, R.M.M., Ferdelman, T.G. and Fabricius, K.E., 2012. Mechanisms of damage to corals exposed to sedimentation. *Proceedings of the National Academy of Sciences of the United States of America,* 109(24), E1558–E1567. 10.1073/pnas.1100715109.

Williams, G.J., Smith, J.E., Conklin, E.J., Gove, J.M., Sala, E. and Sandin, S.A., 2013. Benthic communities at two remote Pacific coral reefs: effects of reef habitat, depth, and wave energy gradients on spatial patterns. *PeerJ*, 1:e81. 10.7717/peerj.81.

Woodroffe, C.D., 2008. Reef-island topography and the vulnerability of atolls to sea-level rise. *Global and Planetary Change*, 62(1-2), pp.77-96. 10.1016/j.gloplacha.2007.11.001.

World Bank, 2013. *Acting on climate change and disaster risk for the Pacific*. [pdf] Washington: World Bank. Available at: <http://documents.worldbank.org/curated/en/354821468098054153/Acting-on-climatechange-and-disaster-risk-for-the-Pacific> [Accessed 6 November 2017].

Yao.Y., Zhang, Q., Chen, S. and Tang, Z., 2019. Effects of reef morphology variations on wave processes over fringing reefs. *Applied Ocean Research*, 82, pp.52-62. 10.1016/j.apor.2018.10.021.

Appendices

Appendix A

Table A.1 – The GPS coordinates of the 16 study sites around the Tarawa and Abaiang Atolls, Kiribati.

Site	Longitude (°N)	Latitude (°E)	Atoll
T02	1.333167	173.0217	South Tarawa
T05	1.6325	172.9673	North Tarawa
T07	1.617783	172.9336	North Tarawa
T08	1.358117	173.1446	South Tarawa
T10	1.3302	172.9634	South Tarawa
T11	1.357	173.079	South Tarawa
T12	1.32455	172.9951	South Tarawa
T13	1.346317	172.9241	South Tarawa
T15	1.350567	173.0466	South Tarawa
T16	1.39105	173.1507	South Tarawa
A01	1.85765	172.8796	Abaiang
A02	1.881967	172.818	Abaiang
A03	1.714333	172.9865	Abaiang
A05	1.920917	172.804	Abaiang
A06	1.897167	172.7772	Abaiang
A11	1.803283	172.9088	Abaiang

Table A.2 – Photomosaic coral cover and environmental data compared across all 16 study sites.

Site	Local human disturbance	Branching coral cover	Massive coral cover	Porites rus coral cover	Avg. depth (m)	Slope of fore reef (°)	CV_{SST} (°C)
T02	7.417	2.756	2.544	12.726	7.93	15.91	0.0211
T08	7.599	3.604	0.474	39.386	9.9	11.42	0.0211
T10	7.556	1.445	0.702	56.407	9.38	13.94	0.0212
T11	8.728	2.784	0.266	43.274	12.58	29.49	0.0211
T12	7.418	2.23	0.321	58.19	9.78	14.22	0.0212
T13	9.473	0.593	1.101	26.474	10.73	9.68	0.0212
T15	8.556	7.117	2.41	20.135	8.97	18.22	0.0212
T16	7.398	13.279	14.66	0.301	9.48	3.85	0.021
T05	5.555	8.95	4.114	0.1	9.22	11.01	0.0212
T07	5.668	5.106	11.957	0.052	9.45	7.71	0.0212
A01	4.072	4.527	18.344	0	9.02	5.47	0.0197
A02	5.952	4.204	5.834	0.009	8.23	15.23	0.0197
A03	5.291	18.776	17.23	0.099	9.38	7.96	0.0197
A05	4.886	33.528	21.421	0.007	9.45	5.59	0.0209
A06	4.978	13.313	17.95	0	9.68	1.22	0.0196
A11	3.37	20.323	14.216	0.065	10.17	7.52	0.0201

Table A.3 – Values of structural complexity metrics compared across sites at the Tarawa and Abaiang Atolls, Kiribati.

Site	Surface rugosity	SDE (m)	Terrain ruggedness
T02	2.278	0.033	0.103
T08	2.954	0.041	0.125
T10	3.342	0.05	0.103
T11	2.404	0.032	0.097
T12	2.644	0.031	0.154
T13	2.383	0.034	0.097
T15	2.84	0.042	0.11
T16	2.71	0.041	0.097
T05	2.475	0.044	0.088
T07	2.257	0.032	0.097
A01	2.235	0.037	0.068
A02	2.024	0.03	0.073
A03	2.723	0.041	0.101
A05	2.571	0.038	0.111
A06	2.547	0.039	0.084
A11	3.339	0.057	0.098

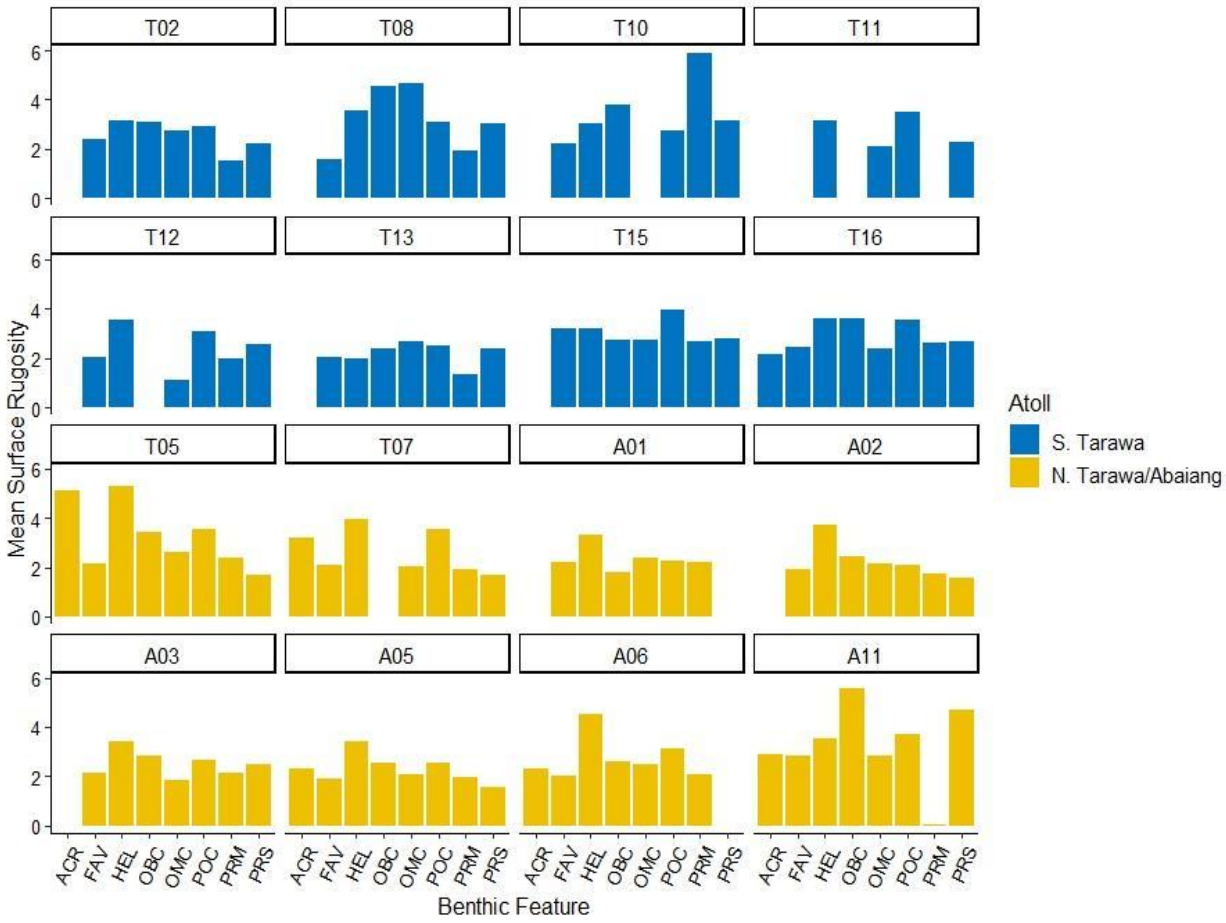

Figure A.1 – Comparisons between the mean surface rugosity of key reef building coral taxa across fore reef sites in Tarawa and Abaiang Atolls, Kiribati. ACR = *Acropora*, FAV = *Favids*, HEL = *Heliopora*, OBC = Other Branching Coral, OMC = Other Massive Coral, POC = *Pocillopora*, PRM = *Porites* Massive, PRS = *Porites rus*.

Table A.4 – Mean surface rugosity of the major reef building corals and sand compared across all 16 study sites. Note: Measurements only recorded for adult coral colonies (i.e. greater than 5 cm in diameter). ACR = *Acropora*, FAV = *Favids*, HEL = *Heliopora*, OBC = Other Branching Coral, OMC = Other Massive Coral, POC = *Pocillopora*, PRM = *Porites* Massive, PRS = *Porites rus*.

	Benthic Feature								
Site	ACR	FAV	HEL	OBC	OMC	POC	PRM	PRS	Sand
T02	—	2.400	3.153	3.121	2.750	2.908	1.528	2.251	—
T08	—	1.584	3.560	4.550	4.662	3.082	1.946	3.011	—
T10	—	2.219	3.050	3.792	—	2.728	5.909	3.150	1.886
T11	—	—	3.181	—	2.126	3.494	—	2.286	—
T12	—	2.031	3.531	—	1.096	3.061	1.969	2.544	—
T13	—	2.066	1.987	2.417	2.678	2.498	1.347	2.411	1.837
T15	—	3.189	3.189	2.756	2.739	3.949	2.685	2.801	—
T16	2.170	2.474	3.629	3.616	2.370	3.569	2.648	2.668	—
T05	5.117	2.170	5.292	3.420	2.623	3.565	2.366	1.686	1.241
T07	3.184	2.117	3.927	—	2.050	3.527	1.902	1.694	—
A01	—	2.196	3.303	1.815	2.390	2.246	2.231	—	1.560
A02	—	1.904	3.715	2.420	2.126	2.097	1.756	1.544	—
A03	—	2.116	3.441	2.842	1.845	2.641	2.110	2.512	—
A05	2.284	1.919	3.416	2.565	2.076	2.523	1.965	1.568	—
A06	2.289	2.007	4.499	2.613	2.474	3.102	2.080	—	1.396
A11	2.918	2.841	3.558	5.563	2.849	3.712	3.255	4.684	1.551

Appendix B

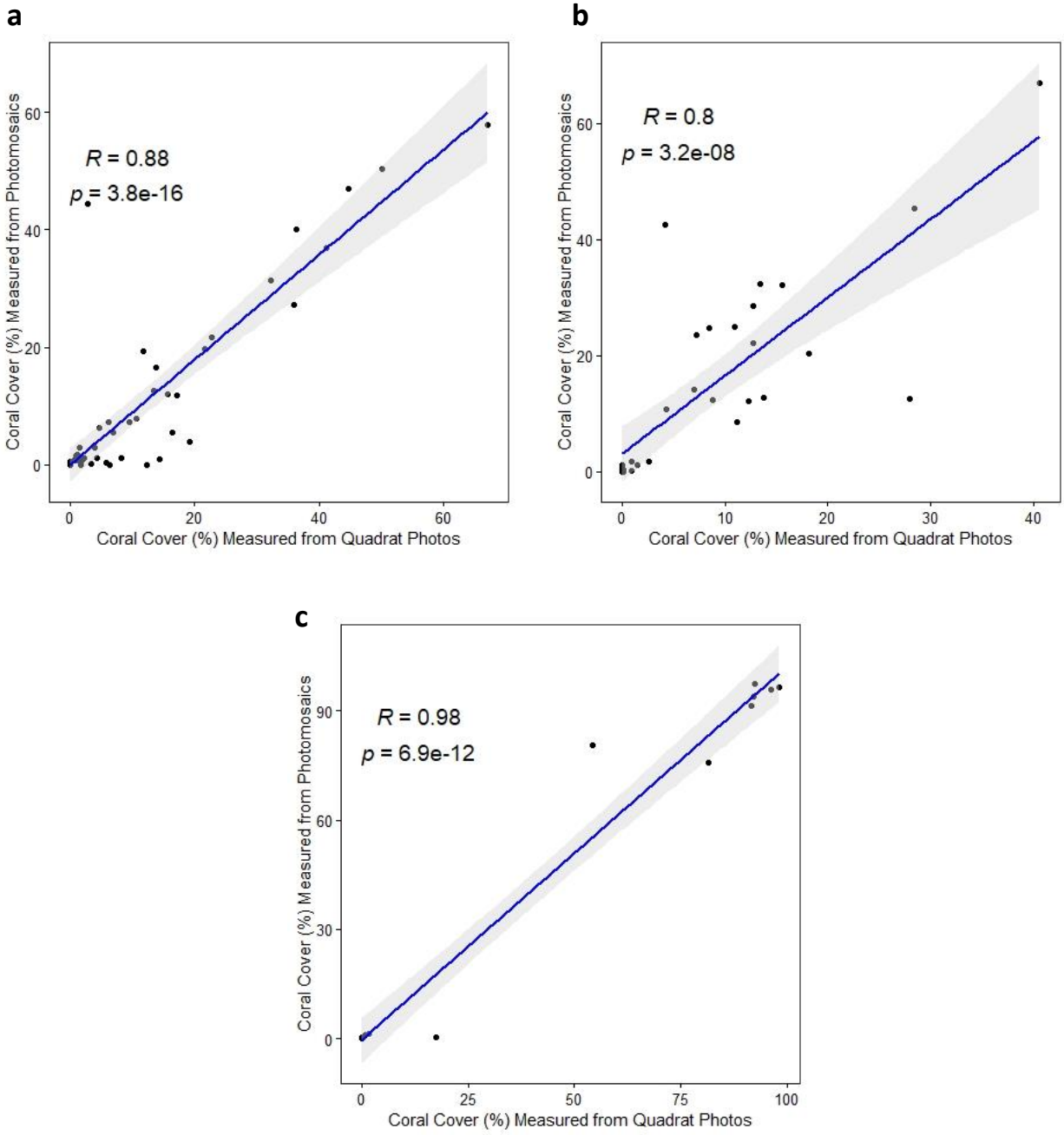

Figure B.1 – Scatter plot of Pearson correlation between coral cover calculated using the quadrat photos and photomosaics at each of the sites and for all three coral morphologies. The three coral morphologies are (a) branching, (b) massive, and (c) *Porites rus*.

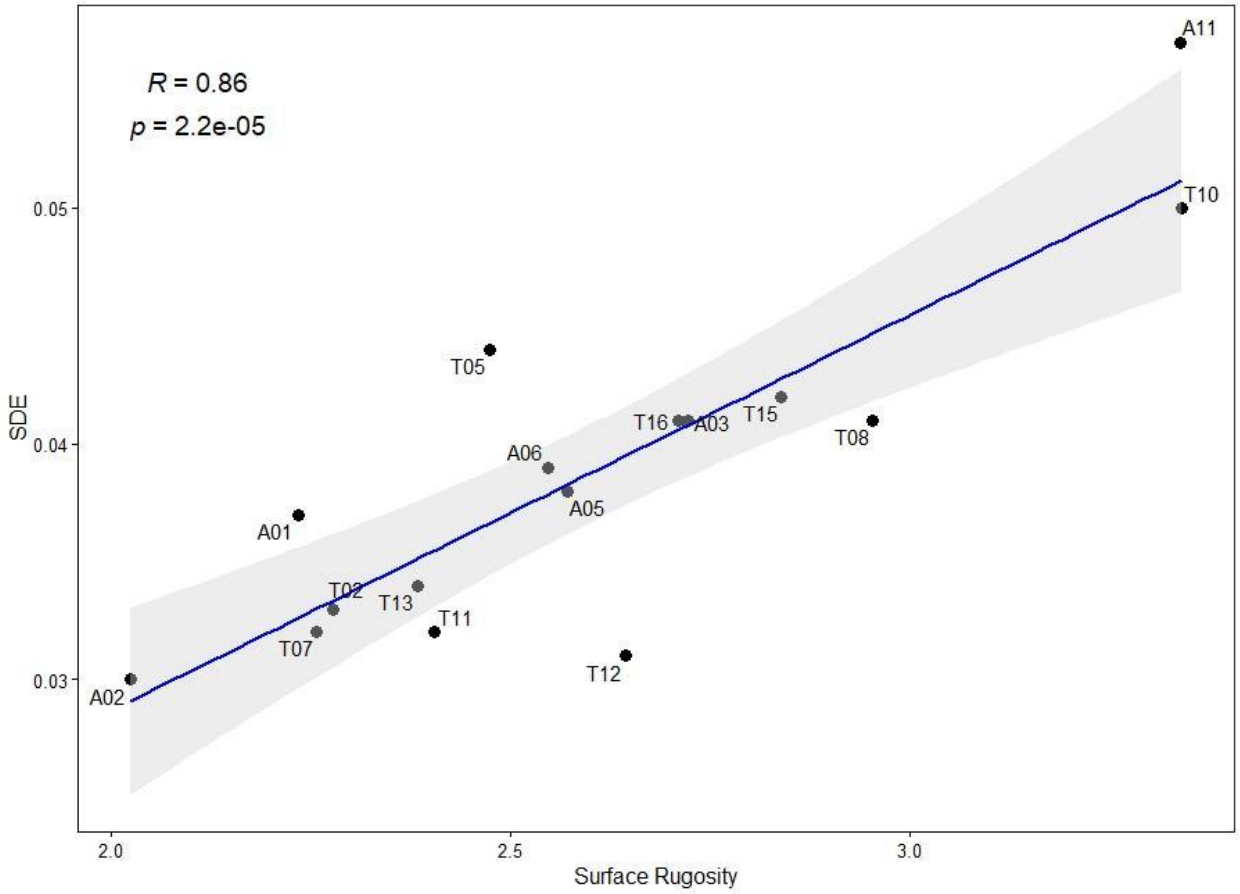

Figure B.2 – Scatter plot of Pearson correlation between the surface rugosity and SDE of the fore reef plots at each of the sites.

Table B.1 – Results of ANOVA of terrain ruggedness.

	Dependent variable: terrain ruggedness				
Independent variable	Df	Sum Sq	Mean Sq	F value	Pr (>F)
atoll	1	0.001722	0.0017222	5.674	0.032 *
Residuals	14	0.004249	0.0003035		
Note:					*p<0.05, **p<0.01, ***p<0.001

Table B.2 – Results of ANOVA of local human disturbance.

	Dependent variable: local human disturbance				
Independent variable	Df	Sum Sq	Mean Sq	F value	Pr (>F)
atoll	1	37.13	37.13	53.72	3.74e-06 ***
Residuals	14	9.68	0.69		
Note:					*p<0.05, **p<0.01, ***p<0.001

Table B.3 – Results of Kruskal-Wallis tests of benthic cover across atolls.

	Independent variable: atoll		
Dependent variable	Kruskal-Wallis chi-squared	Df	p-value
Halimeda	12.884	1	0.0003314 ***
Cyanobacteria	8.8981	1	0.002855 **
Porites rus	12.178	1	0.0004835 ***
Favids	10.158	1	0.001437 **
Note:			*p<0.05, **p<0.01, ***p<0.001

Table B.4 – Results of ANOVA of mean rugosity.

	Dependent variable: mean surface rugosity				
Independent variables	Df	Sum Sq	Mean Sq	F value	Pr (>F)
atoll	1	0.52	0.523	0.778	0.380
morphology	2	22.80	11.399	16.951	5.17e-07 ***
benthic feature	5	2.91	0.582	0.865	0.508
atoll:morphology	2	1.92	0.960	1.427	0.245
atoll:benthic feature	5	4.14	0.829	1.233	0.300
Residuals	94	63.21	0.672		
Note:					*p<0.05, **p<0.01, ***p<0.001

Table B.5 – Results of Tukey HSD test of mean surface rugosity by coral morphology.

	Dependent variable: mean surface rugosity			
	diff	lwr	upr	p adj
Massive – Branching	-0.9480926	-1.3474959	-0.5467345	0.0000005 ***
Porites rus – Branching	-0.7406841	-1.3327845	-0.1485838	0.0101051**
Porites rus –Massive	0.2074085	-0.3931336	0.8079506	0.6909540
Note:				*p<0.05, **p<0.01, ***p<0.001

Appendix C

Table C.1 – Set of reasonably well-fitting models that describe the structural complexity metric surface rugosity. The check marks indicate variables present within each of the models above. Disturbance = local human disturbance; Branching = branching coral cover; Massive = massive coral cover; *Porites rus* = *Porites rus* coral cover; Temperature variability = coefficient of variation of maximum annual SST (CV_{SST}); df = degrees of freedom; AIC_c = Akaike information criteria for small sample sizes; ΔAIC_c = difference from the lowest AIC_c value (i.e. 'best' model), only models with a $\Delta AIC_c < 10$ shown; w = model weight; RVI = relative variable importance. The relative variable importance (RVI) ranges from 0 to 1, with 0 being a parameter that has no importance on the structural complexity metric and 1 being a parameter that is very important to the structural complexity metric.

Rank	Disturbance	Branching	Massive	*Porites rus*	Temperature variability	*df*	AIC_c	ΔAIC_c	*W*
1		✓		✓		5	21.2	0.00	0.217
2				✓		4	22.4	1.24	0.117
3		✓				4	23.6	2.42	0.065
4	✓					4	24.2	2.99	0.049
5				✓	✓	5	24.3	3.12	0.046
6			✓			4	24.5	3.27	0.042
7			✓	✓		5	25.0	3.81	0.032
8					✓	4	25.0	3.85	0.032
9		✓	✓			5	25.4	4.21	0.026
10		✓		✓	✓	6	25.7	4.46	0.023
11	✓	✓		✓		6	26.5	5.27	0.016
12		✓	✓	✓		6	26.5	5.31	0.015
13	✓			✓		5	26.7	5.54	0.014
14	✓	✓				5	27.1	5.85	0.012
15		✓			✓	5	27.8	6.62	0.008
16	✓				✓	5	28.0	6.76	0.007
17	✓		✓			5	28.5	7.32	0.006
18			✓		✓	5	28.6	7.36	0.005
19	✓			✓	✓	6	29.2	7.97	0.004
20			✓	✓	✓	6	29.3	8.11	0.004
21	✓		✓	✓		6	30.2	9.05	0.002
22		✓	✓		✓	6	30.5	9.26	0.002
23	✓	✓	✓			6	30.7	9.54	0.002
RVI	0.13	0.39	0.14	0.49	0.11				

Table C.2 – Set of reasonably well-fitting models that describe the structural complexity metric standard deviation of elevation (SDE). See Table C.1 for an explanation of the variables in the table.

Rank	Disturbance	Branching	Massive	*Porites rus*	Temperature variability	*df*	AIC_c	ΔAIC_c	*W*
1		✓				4	-104.4	0.00	0.170
2	✓					4	-104.2	0.27	0.148
3			✓			4	-102.5	1.91	0.065
4					✓	4	-102.2	2.29	0.054
5				✓		4	-102.1	2.39	0.051
6	✓			✓		5	-100.7	3.72	0.026
7	✓	✓				5	-100.6	3.84	0.025
8		✓	✓			5	-100.6	3.88	0.024
9		✓		✓		5	-100.6	3.88	0.024
10	✓				✓	5	-100.6	3.89	0.024
11	✓		✓			5	-100.2	4.23	0.020
12		✓			✓	5	-100.1	4.36	0.019
13			✓	✓		5	-98.3	6.10	0.008
14			✓		✓	5	-98.2	6.27	0.007
15				✓	✓	5	-97.8	6.65	0.006
16	✓	✓	✓			6	-97.7	6.79	0.006
17	✓	✓		✓		6	-96.9	7.55	0.004
18	✓			✓	✓	6	-95.9	8.54	0.002
19	✓	✓			✓	6	-95.8	8.62	0.002
20		✓	✓		✓	6	-95.5	8.95	0.002
21	✓		✓		✓	6	-95.4	9.01	0.002
22	✓		✓	✓		6	-95.4	9.02	0.002
23		✓	✓	✓		6	-95.3	9.10	0.002
24		✓		✓	✓	6	-95.3	9.12	0.002
RVI	0.261	0.277	0.133	0.124	0.117				

Table C.3 – Set of reasonably well-fitting models that describe the structural complexity metric terrain ruggedness. See Table C.1 for an explanation of the variables in the table.

Rank	Disturbance	Branching	Massive	*Porites rus*	Temperature variability	*df*	AIC_c	ΔAIC_c	*W*
1		✓		✓		5	-79.1	0.00	0.323
2				✓		4	-78.3	0.79	0.217
3		✓		✓	✓	6	-76.5	2.63	0.087
4					✓	4	-75.8	3.33	0.061
5				✓	✓	5	-75.8	3.38	0.060
6		✓	✓	✓		6	-74.7	4.42	0.035
7			✓	✓		5	-74.5	4.62	0.032
8	✓	✓		✓		6	-74.1	5.01	0.026
9	✓			✓		5	-74.1	5.05	0.026
10			✓	✓	✓	6	-72.7	6.46	0.013
11			✓			4	-72.3	6.83	0.011
12	✓					4	-72.1	7.01	0.010
13		✓			✓	5	-72.1	7.02	0.010
14		✓	✓			5	-72.1	7.05	0.010
15	✓			✓	✓	6	-72.1	7.07	0.009
16		✓				4	-71.7	7.42	0.008
17			✓		✓	5	-71.5	7.65	0.007
18	✓				✓	5	-71.4	7.69	0.007
19	✓	✓		✓	✓	7	-70.0	9.13	0.003
20		✓	✓	✓	✓	7	-69.9	9.27	0.003
21	✓		✓	✓		6	-69.2	9.94	0.002
RVI	0.08	0.51	0.11	0.85	0.26				

Table C.4 – Set of reasonably well-fitting models that describe the structural complexity metric surface rugosity. The check marks indicate variables present within each of the models above. Disturbance = local human disturbance; Branching = branching coral cover; Massive = massive coral cover; *Porites rus* = *Porites rus* coral cover; Temperature variability = coefficient of variation of maximum annual SST (CV_{SST}); Water depth = average water depth of the fore reef; df = degrees of freedom; AIC_c = Akaike information criteria for small sample sizes; ΔAIC_c = difference from the lowest AIC_c value (i.e. 'best' model), only models with a $\Delta AIC_c < 10$ shown; w = model weight; RVI = relative variable importance. The relative variable importance (RVI) ranges from 0 to 1, with 0 being a parameter that has no importance on the structural complexity metric and 1 being a parameter that is very important to the structural complexity metric.

Rank	Disturbance	Branching	Massive	*Porites rus*	Temperature variability	Water depth	*df*	AIC_c	ΔAIC_c	*W*
1		✓		✓			5	21.2	0.00	0.193
2				✓			4	22.4	1.24	0.104
3		✓					4	23.6	2.42	0.058
4						✓	4	24.1	2.88	0.046
5					✓		4	24.2	2.99	0.043
6	✓			✓			5	24.3	3.12	0.041
7			✓				4	24.5	3.27	0.038
8			✓	✓			5	25.0	3.81	0.029
9	✓						4	25.0	3.85	0.028
10		✓	✓				5	25.4	4.21	0.024
11	✓	✓		✓			6	25.7	4.46	0.021
12		✓		✓		✓	6	26.3	5.13	0.015
13		✓		✓	✓		6	26.5	5.27	0.014
14		✓	✓	✓			6	26.5	5.31	0.014
15				✓	✓		5	26.7	5.54	0.012
16				✓		✓	5	26.8	5.59	0.012
17		✓			✓		5	27.1	5.85	0.010
18		✓				✓	5	27.5	6.26	0.008
19	✓	✓					5	27.8	6.62	0.007
20	✓				✓		5	28.0	6.76	0.07
21					✓	✓	5	28.2	7.03	0.06
22			✓			✓	5	28.4	7.22	0.05
23			✓		✓		5	28.5	7.32	0.05
24	✓		✓				5	28.6	7.36	0.05
25	✓					✓	5	28.6	7.37	0.05
26	✓			✓	✓		6	29.2	7.97	0.04
27	✓		✓	✓			6	29.3	8.11	0.03
28	✓			✓		✓	6	29.6	8.40	0.03
29			✓	✓	✓		6	30.2	9.05	0.02
30			✓	✓		✓	6	30.3	9.12	0.02
31	✓	✓	✓				6	30.5	9.26	0.02
32		✓	✓			✓	6	30.5	9.35	0.02
33		✓	✓		✓		6	30.7	9.54	0.02
RVI	0.11	0.37	0.13	0.47	0.11	0.10				

Table C.5 – Set of reasonably well-fitting models that describe the structural complexity metric standard deviation of elevation (SDE). See Table C.4 for an explanation of the variables in the table.

Rank	Disturbance	Branching	Massive	*Porites rus*	Temperature variability	Water depth	*df*	AIC_c	ΔAIC_c	*W*
1		✓					4	-104.4	0.00	0.151
2	✓						4	-104.2	0.27	0.132
3			✓				4	-102.5	1.91	0.058
4					✓		4	-102.2	2.29	0.048
5				✓			4	-102.1	2.39	0.046
6						✓	4	-102.0	2.48	0.044
7	✓			✓			5	-100.7	3.72	0.024
8	✓	✓					5	-100.6	3.84	0.022
9		✓	✓				5	-100.6	3.88	0.022
10		✓		✓			5	-100.6	3.88	0.022
11	✓				✓		5	-100.6	3.89	0.018
12	✓		✓				5	-100.2	4.23	0.017
13	✓					✓	5	-100.1	4.32	0.017
14		✓				✓	5	-100.1	4.35	0.017
15		✓			✓		5	-100.1	4.36	0.007
16			✓	✓			5	-98.3	6.10	0.007
17			✓			✓	5	-98.2	6.23	0.007
18			✓		✓		5	-98.2	6.27	0.007
19					✓	✓	5	-97.8	6.63	0.005
20				✓	✓		5	-97.8	6.65	0.005
21				✓		✓	5	-97.7	6.72	0.005
22	✓	✓	✓				6	-97.7	6.79	0.005
23	✓	✓		✓			6	-96.9	7.55	0.003
24	✓			✓	✓		6	-95.9	8.54	0.002
25	✓	✓			✓		6	-95.8	8.62	0.002
26	✓				✓	✓	6	-95.5	8.92	0.002
27		✓	✓		✓		6	-95.5	8.95	0.002
28	✓			✓		✓	6	-95.5	8.96	0.002
29	✓	✓				✓	6	-95.5	8.99	0.002
30	✓		✓		✓		6	-95.4	9.01	0.002
31	✓		✓	✓			6	-95.4	9.02	0.002
32		✓	✓	✓			6	-95.3	9.10	0.002
33		✓		✓	✓		6	-95.3	9.12	0.002
34	✓		✓			✓	6	-95.3	9.17	0.002
35		✓		✓		✓	6	-95.3	9.18	0.002
36		✓	✓			✓	6	-95.2	9.21	0.002
37		✓			✓	✓	6	-94.8	9.68	0.001
RVI	0.253	0.268	0.126	0.117	0.111	0.098				

Table C.6 – Set of reasonably well-fitting models that describe the structural complexity metric terrain ruggedness. See Table C.4 for an explanation of the variables in the table.

Rank	Disturbance	Branching	Massive	*Porites rus*	Temperature variability	Water depth	*df*	AIC_c	ΔAIC_c	*W*
1		✓		✓			5	-79.1	0.00	0.286
2				✓			4	-78.3	0.79	0.192
3		✓		✓	✓		6	-76.5	2.63	0.077
4					✓		4	-75.8	3.33	0.054
5				✓	✓		5	-75.8	3.38	0.053
6		✓		✓		✓	6	-75.6	3.53	0.049
7		✓	✓	✓			6	-74.7	4.42	0.031
8			✓	✓			5	-74.5	4.62	0.028
9				✓		✓	5	-74.3	4.78	0.026
10	✓	✓		✓			6	-74.1	5.01	0.023
11	✓			✓			5	-74.1	5.05	0.023
12			✓	✓	✓		6	-72.7	6.46	0.011
13			✓				4	-72.3	6.83	0.009
14	✓						4	-72.1	7.01	0.009
15		✓			✓		5	-72.1	7.02	0.009
16		✓	✓				5	-72.1	7.05	0.008
17	✓			✓	✓		6	-72.1	7.07	0.008
18		✓		✓	✓	✓	7	-72.0	7.10	0.008
19		✓					4	-71.7	7.42	0.007
20			✓		✓		5	-71.5	7.65	0.006
21					✓	✓	5	-71.4	7.68	0.006
22	✓				✓		5	-71.4	7.69	0.006
23				✓	✓	✓	6	-70.8	8.28	0.005
24						✓	4	-70.8	8.28	0.005
25	✓	✓		✓	✓		7	-70.0	9.13	0.003
26		✓	✓	✓	✓		7	-69.9	9.27	0.003
27			✓	✓		✓	6	-69.8	9.32	0.003
28		✓	✓	✓		✓	7	-69.7	9.39	0.003
29	✓	✓		✓		✓	7	-69.6	9.51	0.002
30	✓		✓	✓			6	-69.2	9.94	0.002
RVI	0.08	0.52	0.11	0.85	0.25	0.11				